

High-precision Monte Carlo study of universal correlation lengths scaling in three-dimensional $O(n)$ spin models

Martin Weigel* and Wolfhard Janke†

Institut für Theoretische Physik, Universität Leipzig, 04109 Leipzig, Germany

(Dated: October 22, 2019)

Using an elaborate set of simulational tools and statistically optimized methods of data analysis we investigate the scaling behavior of the correlation lengths of three-dimensional classical $O(n)$ spin models. Considering three-dimensional slabs $S^1 \times S^1 \times \mathbb{R}$, the results over a wide range of n indicate the validity of special scaling relations involving universal amplitude ratios that are analogous to results of conformal field theory for two-dimensional systems. A striking mismatch of the $n \rightarrow \infty$ extrapolation of these simulations against analytical calculations is traced back to a breakdown of the identification of this limit with the spherical model.

PACS numbers: 64.60.Fr, 75.10.Mk, 75.40.Mg, 11.25.Hf

I. INTRODUCTION

The concept of scaling, the observation that singular observables vary in a scale-free manner according to power laws when the driving parameter of a transition (temperature, magnetic field, ...) is tuned towards a critical point, has since the first observations been a key ingredient of the theory of critical phenomena^{1,2}. Exploiting the symmetry of scale-invariance forming the geometrical basis for the power-law behavior in the vicinity of a critical point through the idea of real-space normalization, scaling theory can be mapped on the behavior of finite systems near the transition point of the bulk system in the limit of diverging system sizes, the thermodynamic limit. This *finite-size scaling* (FSS)^{3,4,5} occurs with scaling exponents generically linked to the exponents that govern scaling in the bulk system. Thus the apparent weakness of finite system size that hampers simulational approaches actually turns out to be their intrinsic strength, when exploring FSS means exploring thermal scaling^{6,7}.

The significance of scaling theory for the understanding of critical phenomena becomes quite exposed in the context of conformal field theory (CFT) for two-dimensional systems⁸. In the course of exploiting the additional invariances of conformal symmetry one is able to split the critical point partition function of a lattice system into a sum over contributions from all the scaling variables present in a specific model. Consider a critical system on a $L \times L'$ lattice with toroidal boundary conditions; then the partition function decomposes as^{9,10}:

$$Z(L, L') = e^{-fA + \pi c \delta / 6} \sum_n e^{-2\pi x_n \delta}, \quad (1)$$

where c is the central charge of the considered theory, f the bulk free energy per unit volume, $\delta = L'/L$, $A = LL'$, and the sum runs over the whole content of scaling operators with dimensions x_n . Thus, the knowledge of the operator content of a theory in connection with the corresponding scaling dimensions is equivalent to an “exact” solution of the model on finite lattices.

Two Dimensions – A particular example of a scaling relation in two dimensions that can be derived assuming conformal invariance of critical point entities concerns the two-point function in the limit of $L' \rightarrow \infty$. It is generally sufficient to assume translational, rotational, dilatational, and inversive invariance to imply conformal invariance¹¹; homogeneity, isotropy and scale invariance alone suffice to uniquely fix the critical, connected two-point function of an operator ϕ in the infinite plane up to an overall normalization factor:

$$\langle \phi(z_1, \bar{z}_1) \phi(z_2, \bar{z}_2) \rangle_c = (z_1 - z_2)^{-x} (\bar{z}_1 - \bar{z}_2)^{-x}, \quad (2)$$

where z_1, z_2 are complex co-ordinates parametrizing the plane. Then, one uses the logarithmic map

$$w = \frac{L}{2\pi} \ln z, \quad z \in \mathbb{C} \quad (3)$$

to wrap the complex plane around an infinite length cylinder $S^1 \times \mathbb{R}$ of circumference L with co-ordinates $w = u + iv$, where v measures the polar angle along S^1 and u the longitudinal direction along \mathbb{R} . Assuming conformally covariant transformation behavior of the (primary) operator ϕ , one arrives at an expression for the two-point function on the cylinder¹²:

$$\langle \phi(w_1, \bar{w}_1) \phi(w_2, \bar{w}_2) \rangle_c = \left(\frac{2\pi}{L} \right)^{2x} \left(\frac{|z_1 z_2|}{|z_1 - z_2|^2} \right)^x = \left(\frac{2\pi}{L} \right)^{2x} \left(2 \cosh \frac{2\pi}{L} (u_1 - u_2) - 2 \cos \frac{2\pi}{L} (v_1 - v_2) \right)^{-x} \quad (4)$$

In the limit of large longitudinal distances $|u_1 - u_2| \gg L$ and $v_1 = v_2$, one is left with a purely exponential drop with a correlation length

$$\xi_{\parallel} = \frac{L}{2\pi x}. \quad (5)$$

Thus, utilization of conformal invariance yields a finite-size scaling relation *including the amplitude*, which is in contrast to renormalization group theory that usually gives the scaling exponents and only certain amplitude

ratios, but not the amplitudes themselves. Since this result emerges from a field-theoretic description of statistical mechanics that does not take into account the microscopical details of the system, like the exact form of interactions (apart from their locality) and lattice arrangement, this result is expected to be *universal*, i.e. valid irrespective of those details¹³. Note, however, that this proposed universality goes beyond the usual notion of an universal quantity and comprises three different aspects: (i) the correlation length of a given operator should be the same within the associated universality class of models; (ii) when looking at different operators, on the other hand, the form of Eq. (5) should be left unchanged, all operator-dependent information being condensed in the scaling dimension x ; (iii) finally, even when looking at models of *different* universality classes, all that should change are the scaling dimensions (and the definition of ϕ), the validity of Eq. (5) being untouched. Property (i) implies the “hyperuniversality” relation of Privman and Fisher¹⁴. In the following, we will refer to the whole extent of aspects (i)-(iii) exceeding the usual notion of universality with the term “hyperuniversal”. A corollary that is of importance for transfer matrix calculations that use an unnormalized (quantum) Hamiltonian results from taking the ratio of the correlation lengths of two primary operators, for example the densities of magnetization and energy which are usually primary for spin models:

$$\frac{\xi_\sigma}{\xi_\epsilon} = \frac{x_\epsilon}{x_\sigma}. \quad (6)$$

Because of the independence from the overall amplitude $1/2\pi$ of Eq. (5) this relation might still stay valid when changing the geometry in a way such that only this overall amplitude is altered. In terms of universality this constitutes a weaker form of the aspect (i) above, namely universality of amplitude ratios instead of amplitudes themselves; we will refer to this weaker property as (i') in the following.

A suitable test-bed for these general field-theory results is, of course, given by the exactly solvable two-dimensional Ising model. Using Eq. (5) and the generic relations between scaling dimensions and the conventional critical exponents:

$$x_\epsilon = \frac{1-\alpha}{\nu}, \quad x_\sigma = \frac{\beta}{\nu}, \quad (7)$$

giving $x_\sigma = 1/8$ and $x_\epsilon = 1$ for the two-dimensional Ising model, one arrives at a ratio $x_\epsilon/x_\sigma = 8$. A direct evaluation of the spin-spin correlation length in the Onsager-Kaufman framework gives, as the leading term in the scaling series, $\xi_\sigma = 4L/\pi \equiv L/(2\pi\frac{1}{8})$, in agreement with the CFT result^{15,16,17}. The same holds true for the leading scaling amplitude of the energy-energy correlation function¹⁸, $\xi_\epsilon = L/2\pi$. Both amplitudes have also been evaluated numerically to high precision in a Monte Carlo (MC) study¹⁹, resulting in perfect agreement with Eq. (5). A possible alteration of the $S^1 \times \mathbb{R}$ situation, namely

changing the boundary conditions along the S^1 -direction from periodic to *antiperiodic* has also been treated within the CFT framework, exploiting the fact that in the case of the ferromagnetic nearest-neighbor Ising model the antiperiodic boundary corresponds to the insertion of a seam of *antiferromagnetic* bonds along this boundary line. This calculation yields^{20,21}:

$$\begin{aligned} \xi_\sigma &= \frac{4}{3\pi}L, \\ \xi_\epsilon &= \frac{1}{4\pi}L, \end{aligned} \quad (8)$$

again in good agreement with Monte Carlo data¹⁹. Note, however, that this last relation, in contrast to Eq. (5), is specific to the Ising model *and* the special choice of the densities of magnetization and energy as operators and thus is not “hyperuniversal” in the sense of properties (ii) and (iii) presented above.

The amplitude-exponent relation Eq. (5) for two-dimensional systems has been checked analytically or numerically and found valid for an impressive series of further models like the Potts model and its percolation limit¹⁷, the XY model²², the symmetric eight-vertex model¹⁸, and quantum spin models²³ to name only the most prominent.

Three Dimensions – On leaving the domain of two-dimensional systems towards higher dimensions, the wealth of exact field theoretic calculations is instantly reduced to severe scarcity. The conformal group coincides with the algebra of holomorphic functions in the special case of spatial dimension $d = 2$ and is thus infinite-dimensional as a group. For $d \geq 3$, unfortunately, it reduces to a simple Lie group with dimension $D \leq (d+1)(d+2)/2$ for any Riemannian, connected manifold²⁴. In Euclidean spaces it is generated by Euclidean transformations, dilatations with a constant factor, and inversion maps²⁵. As a consequence, only in two dimensions the postulate of conformal invariance is restrictive enough for a classification of the operator contents of the different universality classes and thus an exact solution of the critical theories within the limits of field-theory assumptions. For $d \geq 3$, on the other hand, the implications of the finite-dimensional conformal group symmetry reach hardly beyond the consequences of plain renormalization group theory exploiting dilatational symmetry. However, since inversional symmetry is still present, some generalization on analytical grounds of Eq. (5) to higher dimensions is nevertheless possible. Rewriting the logarithmic map Eq. (3) in polar co-ordinates its operation only on the radial part becomes explicit; the angular co-ordinate is not affected. It is therefore straightforward to generalize this map to dimensions $d \geq 3$ by simply substituting the respective angular part. This results in a map which is still conformal, now connecting the spaces \mathbb{R}^d and $S^{d-1} \times \mathbb{R}$. Applied to the two-point function one arrives at a scaling relation

analogous to Eq. (5), namely²⁶:

$$\xi_{\parallel} = \frac{R}{x}, \quad (9)$$

which contains the $d = 2$ result as a special case assuming $L = 2\pi R$, R being the radius of S^{d-1} . Note, however, that it no longer follows trivially for which operators ϕ this kind of relation should hold true since “primarity”, i.e. conformal covariance, is *a priori* not well defined for $d \geq 3$. Considering the lack of exact results for three-dimensional systems, especially concerning amplitudes, this is still a quite remarkable result. Numerical tests of this conjecture are hampered, though, by the fact that S^{d-1} for $d \geq 3$ is a truly curved space and thus hard to regularize by discrete lattices. This problem will not be considered here, but instead in a separate publication²⁷.

On the other hand, the toroidal geometry $S^1 \times \dots \times S^1 \times \mathbb{R}$, which is much more convenient for numerical simulations, is not conformally flat and thus no CFT predictions exist for this case. In spite of this theoretically unfavorable situation a transfer matrix calculation for the Hamiltonian limit of the three-dimensional Ising model on the geometry $S^1 \times S^1 \times \mathbb{R} \equiv T^2 \times \mathbb{R}$ by Henkel^{28,29,30} rendered results still comparable to the situation for the $S^{d-1} \times \mathbb{R}$ geometry. For the ratios of leading scaling amplitudes of correlation lengths for different boundary conditions (bc) he found

$$\begin{aligned} \xi_{\sigma}/\xi_{\epsilon} &= 3.62(7) & \text{for periodic bc,} \\ \xi_{\sigma}/\xi_{\epsilon} &= 2.76(4) & \text{for antiperiodic bc.} \end{aligned} \quad (10)$$

A comparison with the (inverse) ratio of corresponding scaling dimensions,

$$x_{\epsilon}/x_{\sigma} = \frac{(1-\alpha)/\nu}{\beta/\nu} = \frac{2(\nu d - 1)}{\nu d - \gamma} = 2.7326(16), \quad (11)$$

(cp. Table I and Eq. (7)) showed that even though the original expectation to possibly find agreement in the case of periodic boundary conditions as in the two-dimensional case was not met, the data are consistent with the relation Eq. (6) for the unorthodox case of *antiperiodic* boundary conditions. Note that one has to compare *ratios* in this case, because the quantum Hamiltonian used in the calculation is defined only up to an overall normalization constant. This result is in qualitative agreement with a Metropolis MC simulation by Weston³¹, who found:

$$\begin{aligned} \xi_{\sigma}/\xi_{\epsilon} &\approx 3.7 & \text{for periodic bc,} \\ \xi_{\sigma}/\xi_{\epsilon} &\approx 2.6 & \text{for antiperiodic bc.} \end{aligned} \quad (12)$$

Considering these striking observations it seems interesting to check whether this behavior is just a coincidence or special feature of the Ising model or instead indicates a general property of critical models on this special three-dimensional geometry.

The rest of the paper is organized as follows. In Sec. II we introduce the general class of models we want to examine and present the way we are going to discretize the

three-dimensional geometry $T^2 \times \mathbb{R}$. We discuss simulation methods, observables, estimators for measurement and parameters of the simulations. In Sec. III we outline the statistical tools used for the data analysis. It is quite hard to extract high-precision information about correlation lengths from MC simulation data; we will thus discuss the special path of data analysis we are going to proceed along and present details of the statistical tools used there for. This tool-set is “calibrated” with simulations of the *two-dimensional* Ising model, where exact results for comparison are available. In Sec. IV we discuss the results for the correlation lengths ratios of our simulations for the Ising, XY and (generalized) Heisenberg models. Our results, already briefly announced in Ref.³², confirm Henkel’s findings on a high level of accuracy. Furthermore this behavior seems to carry through for the whole class of $O(n)$ spin models and is thus far from being a “numerical accident”. In Sec. V we try to rank our numerical findings in the context of the classification of universality presented above. The type of the model considered enters not only via a variation of the scaling dimensions, but also influences the overall prefactor of Eq. (5). Sec. VI is devoted to the discussion of the relation of our finite- n results to the spherical model, which is connected to the limit $n \rightarrow \infty$ of the class of $O(n)$ spin models. The classic identification of both models seems to break down as soon as (multi-point) correlation functions are considered. The final Sec. VII contains our conclusions.

II. MODELS AND SIMULATION

Throughout this paper we consider zero-field, classical $O(n)$ symmetric spin models with Hamiltonian

$$\mathcal{H} = -J \sum_{\langle ij \rangle} \boldsymbol{\sigma}_i \cdot \boldsymbol{\sigma}_j, \quad \boldsymbol{\sigma}_i \in S^{n-1}, \quad (13)$$

where $J > 0$ resulting in ferromagnetic interactions and the sum $\langle ij \rangle$ is meant to cover pairs of nearest-neighbor spins. The underlying lattice is taken to be simple cubic with dimensions $L_x \times L_y \times L_z$. Special cases of this class of models include the Ising ($n = 1$), XY ($n = 2$), and Heisenberg ($n = 3$) models. This Hamiltonian has the advantage of representing a whole class of models with critical points in three dimensions, tuned by the single parameter n . On the contrary, in two dimensions only the $n = 1$ Ising case exhibits a second order transition, while the models with $n > 2$ do not show separate temperature-dependent phases. The $n = 2$ case exhibits a special, “marginal” phase transition of infinite order of the Kosterlitz-Thouless type. According to the $T^2 \times \mathbb{R}$ geometry we set $L_x = L_y$ and apply periodic *or* antiperiodic boundary conditions in the x and y directions. In both cases we use periodic boundary conditions in the z -direction to eliminate surface effects that are also absent in the $L_z \rightarrow \infty$ case assumed in Eq. (4). To reduce

TABLE I: Literature estimates for the critical exponents ν and γ of the three-dimensional Ising model.

Method	ν	γ
g-expansion ^{33,34}	0.6300(15)	1.241(2)
ϵ -expansion ³⁵	0.6310(15)	1.2390(25)
R.G. FD perturb. ³⁶	0.6301(10)	1.2378(25)
series ³⁷	0.631(4)	1.239(3)
series bcc ³⁸	0.632(1)	1.2395(4)
series bcc ³⁹	0.6300(15)	1.237(2)
series sc ⁴⁰	0.6315(8)	1.2388(10)
series bcc ⁴⁰	0.6308(5)	1.2384(6)
MC ⁴¹	0.6289(8)	1.239(7)
MC ⁴²	0.6301(8)	1.237(2)
weighted mean	0.63055(28)	1.23905(30)

effects of finite size in z -direction one has to ensure that $L_z \gg \xi_{||}$, a concrete rule will be given below.

Since all simulations should be performed as close as possible to the bulk critical temperature, local-update MC simulations would be severely affected by critical slowing down⁴³. We therefore make use of cluster update algorithms that are available beside others for all models of the $O(n)$ symmetry class^{44,45}. Since it is known that at least for systems with aspect ratio close to one Wolff's single cluster variant⁴⁶ performs better than the Swendsen-Wang update in terms of dynamical critical exponents⁴⁷, we used this former variant for all $O(n)$ model simulations. The adaption of this update procedure to the case of antiperiodic boundary conditions along the torus directions is straightforward if one exploits the above mentioned equivalence of an antiperiodic boundary to the insertion of a seam of antiferromagnetic bonds along the boundary line for the case of nearest-neighbor interactions. Considering the Ising model or, alternatively, embedded Ising spins for $n > 1$ models⁴⁵, this means: adjacent spins interacting antiferromagnetically are connected with a bond obeying the Swendsen-Wang probability $p = 1 - \exp(-2\beta J)$ in case of *opposite* orientation and are left unbonded in case of identical orientation. This rule exactly reflects the change in energy compared to the ferromagnetic case and thus trivially satisfies detailed balance.

The main observables of our simulations are the connected correlation functions of the densities of magnetization and energy:

$$\begin{aligned} G_{\sigma}^c(\mathbf{x}_1, \mathbf{x}_2) &= \langle \boldsymbol{\sigma}(\mathbf{x}_1) \cdot \boldsymbol{\sigma}(\mathbf{x}_2) \rangle - \langle \boldsymbol{\sigma} \rangle \cdot \langle \boldsymbol{\sigma} \rangle, \\ G_{\epsilon}^c(\mathbf{x}_1, \mathbf{x}_2) &= \langle \epsilon(\mathbf{x}_1) \epsilon(\mathbf{x}_2) \rangle - \langle \epsilon \rangle \langle \epsilon \rangle. \end{aligned} \quad (14)$$

We define the energy density as a local sum over the neighborhood of a spin:

$$\epsilon(\mathbf{x}) = -\frac{J}{2} \sum_{\mathbf{x}' \text{ nn } \mathbf{x}} \boldsymbol{\sigma}(\mathbf{x}) \cdot \boldsymbol{\sigma}(\mathbf{x}'), \quad (15)$$

the factor $1/2$ ensuring that $E = \sum_{\mathbf{x}} \epsilon(\mathbf{x})$. It is straightforward to construct a bias-reduced estimator for the case of $(\mathbf{x}_2 - \mathbf{x}_1) \parallel \hat{e}_z$, corresponding to the correlation length $\xi = \xi_{||}$: first, taking advantage of the translation invariance of the systems along the z -axis established by a periodic boundary, one can average over the “layers” $i \equiv |z_2 - z_1| = \text{const.}$ To improve on that consider a “zero-mode projection”⁴⁸, i.e. define layered variables

$$\bar{\mathcal{O}}_t(z) = \frac{1}{L_x L_y} \sum_{\mathbf{x}', z'=z} \mathcal{O}_t(\mathbf{x}'), \quad (16)$$

where $\mathcal{O}_t = \boldsymbol{\sigma}_t$ or ϵ_t denotes the times series of MC measurements, and consider the estimator

$$\begin{aligned} \hat{G}_{\mathcal{O}}^{c,||}(i) &= \frac{1}{T} \sum_{t=1}^T \frac{1}{L_z} \sum_{|z_2 - z_1|=i} \bar{\mathcal{O}}_t(z_1) \bar{\mathcal{O}}_t(z_2) \\ &\quad - \left(\frac{1}{T L_z} \sum_{t=1}^T \sum_z \bar{\mathcal{O}}_t(z) \right)^2, \end{aligned} \quad (17)$$

where T denotes the length of the MC time series. This estimator obviously does not directly measure $G^{c,||}$, but inspecting the continuum form Eq. (4) reveals that the deviation stemming from transversal cross-correlations entering the estimator declines exponentially with increasing longitudinal distance i and thus becomes irrelevant for the long-distance behavior we are interested in. Numerical investigations confirm that these considerations stay correct when passing to three dimensions¹⁹. In the large-distance regime zero-mode projection reduces the variance of correlation function estimates by a factor inversely proportional to the layer volume $L_x L_y$. Note that the given estimator for the disconnected part $\langle \mathcal{O} \rangle^2$ has a bias that vanishes as $1/T$ in the large- T limit.

As mentioned above, periodic boundary conditions in z -direction eliminate surface effects associated with this direction, but still effects of finite L_z will trigger deviations from the $L_z \rightarrow \infty$ limit assumed in Eq. (5). Inspecting the form of Eq. (4) in the limit of distances $i \gg \xi_{||}$ one expects longitudinal correlations according to:

$$G^{c,||}(i) \propto e^{-i/\xi_{||}} + e^{-(L_z-i)/\xi_{||}}, \quad (18)$$

i.e. the exponential decay is superimposed by an exponentially increasing part. Thus, using too small values of L_z results in an effective underestimation of correlation lengths. In order to satisfy $L_z \gg \xi_{||}$ in a systematic way, i.e. to keep this effect away from the region of clear signal for measuring the correlation lengths, and assuming linear scaling of correlation lengths according to $\xi_{||} = A L_x$, one has to keep the ratio $L_z/\xi_{||} = L_z/A L_x$ fixed and therefore has to scale L_z proportionally to L_x . Simulations for the case of the *two-dimensional* Ising model show that these finite-size effects are negligible compared to the statistical errors for $L_z/\xi_{||} \gtrsim 10$ and lengths of time series of about 10^6 to 10^7 measurements¹⁹. Adding a safety margin the longitudinal system sizes for the

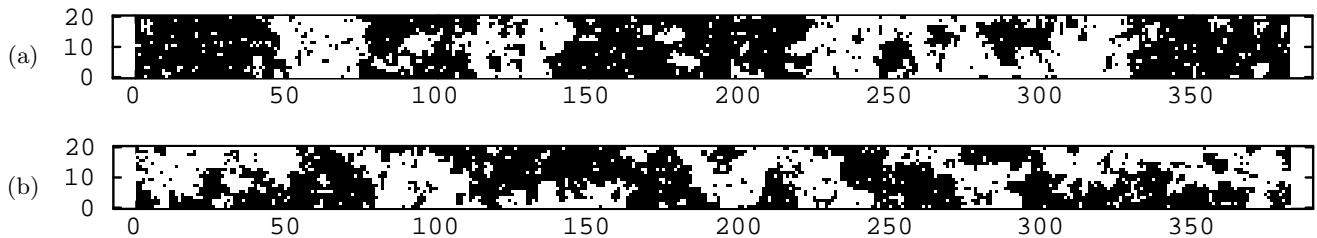


FIG. 1: Typical spin configurations for the two-dimensional Ising model on strips of size 20×382 . (a) periodic boundary conditions; (b) antiperiodic boundary conditions. Note that the visible geometric clusters differ from the stochastic clusters of the cluster update algorithm.

simulations in three dimensions where chosen such that $L_z/\xi_{\parallel} \approx 15$, the scaling amplitude A being estimated from a simulation of an “oversized” system. Since $\xi_{\sigma} > \xi_{\epsilon}$ for all models under consideration, the amplitude A_{σ} of the spin-spin correlation length scaling is significant for the satisfaction of this condition. Note that from Eq. (17) increasing L_z also has the positive side effect of improving the statistics of the correlation function estimation.

In order to judge the efficiency of the used cluster update algorithm and to ensure reasonable usage of computer time we evaluated integrated autocorrelation times

$$\tau_{\text{int}} \equiv \frac{1}{2} + \sum_{\Delta t=1}^{n-1} \frac{\gamma_{\Delta t}}{\gamma_0} \left(1 - \frac{\Delta t}{n}\right), \quad (19)$$

using a binning technique⁴⁹, where γ denotes the unnormalized autocorrelation matrix. The strong asymmetry of the model lattices reduces the average size of clusters and thus Wolff’s cluster update algorithm does not perform as good as on cubic lattices, resulting in increased autocorrelation times. They range up to several hundred Wolff cluster steps for the largest systems considered here; since measurements of $\hat{G}^{c,\parallel}$ are computationally expensive compared to update steps, but the statistical gain vanishes with increasing τ_{int} , measurements were done with frequencies of about $1/\tau_{\text{int}}$. Approaching the low-temperature phase, antiperiodic boundary conditions in the torus directions produce a spatially stable boundary of the geometric clusters along the antiferromagnetic seam, which in turn enforces a second boundary along the z direction. This results in a further reduction of the average cluster size compared to the periodic boundary case. Fig. 1 shows typical configurations for the case of the (two-dimensional) Ising model.

III. DATA ANALYSIS

Having sampled correlation functions using the estimator Eq. (17), a straightforward way to extract an estimate for the correlation lengths is given by a non-linear three-parameter fit of the data to the functional form

$$G^{c,\parallel}(i) = a \exp(-i/\xi_{\parallel}) + b, \quad (20)$$

where, as numerical observations reveal, the additive constant b that enforces non-linearity of the fit, has to be included due to the fact that any estimation of a connected correlation function from a finite-length time series will necessarily fail to reproduce the limit $G(i) \rightarrow 0$ as $i \rightarrow \infty$ exactly because of its finite variance. Thus assuming $b = 0$ *a priori* triggers systematical errors in the correlation length estimation. However, since non-linear fits are intrinsically much less stable than linear fits, not fixing b has severe negative consequences for the stability and statistical error of the resulting correlation length estimate. Since, on the other hand, the constants a and b are irrelevant parameters for our purpose, we propose the following correlation length estimator:

$$\hat{\xi}_{\mathcal{O}}(i) = \Delta \left[\ln \frac{\hat{G}_{\mathcal{O}}^{c,\parallel}(i) - \hat{G}_{\mathcal{O}}^{c,\parallel}(i - \Delta)}{\hat{G}_{\mathcal{O}}^{c,\parallel}(i + \Delta) - \hat{G}_{\mathcal{O}}^{c,\parallel}(i)} \right]^{-1}, \quad (21)$$

which, as insertion of Eq. (20) shows, eliminates the additive and multiplicative constants a and b present in the correlation function estimates. Apart from stability considerations this approach allows for computational simplifications, since correlation functions can be sampled irrespective of normalization and the biased estimation of the disconnected part $\langle \mathcal{O} \rangle^2$ can be dropped. In addition, Eq. (21) simplifies the distinction of the long-distance part of the correlation function from the short-distance region: as the explicit two-dimensional expression Eq. (4) implies, exponential decay will only occur asymptotically, but with deviations decaying themselves exponentially; apart from that, lattice artefacts that are not reflected in the continuum expression Eq. (4) additionally distort the short-distance behavior. Fig. 2 shows an example plot of the spin-spin correlation length estimates $\hat{\xi}_{\sigma}(i)$ for the Ising model. The transition from the short-distance region that should not be used for the final estimate to the purely exponential long-distance behavior is clearly visible. The parameter Δ in Eq. (21) can be used to tune the signal-noise ratio for the correlation length estimate; increasing Δ dramatically reduces the apparent statistical fluctuations in $\hat{\xi}(i)$, cp. Fig. 2. Note, however, that the reduction of variances for individual distances i is accompanied by an increase of cross-correlations between estimates for adjacent estimates, so that the error of an

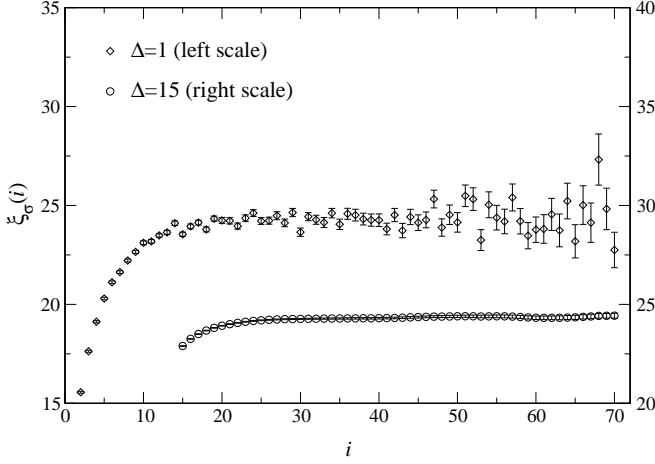


FIG. 2: Correlation length estimates according to Eq. (21) and $\mathcal{O} = \sigma$ for a $30^2 \times 382$ Ising system with periodic boundary conditions for two choices of the typical distance Δ . The plateau regimes collapse if both y axes are scaled identically.

average over a region of distances becomes minimal for an intermediate value of Δ , and not for its maximally allowed value. As a compromise, we use $\Delta \approx 2\xi_\epsilon$ for both estimators $\hat{\xi}_\sigma(i)$ and $\hat{\xi}_\epsilon(i)$.

Naive estimates for the statistical errors (variances) of complex, non-linear combinations of observable measurements like the estimator Eq. (21) are extremely biased due to two effects: even for quite sparse measurements with frequencies around $1/\tau_{\text{int}}$ successive elements of the time series are still correlated, generically leading to systematic underestimation of variances. This effect is being eliminated by the grouping together of measurements to sub-averages of length μ (“binning”)⁴⁹, which leads to an asymptotically uncorrelated time series of length $T' = T/\mu$ used in the further process of error estimation. For the production-run time-series the bin size was chosen to regularly include several thousand measurements, which is far in the asymptotical regime. Secondly, the strong non-linearity of estimators like Eq. (21) forbid the use of the usual formula for the standard deviation of a set of measurements. A common solution to this problem is the use of the Gaussian error propagation formula, which, however, only uses a lowest order Taylor series approximation to the functions and assumes Gaussian distribution of the mean values, i.e. long enough time series for all observables. A far more general ansatz is given by resampling techniques such as the “jackknife”⁵⁰ that apply to a quite general set of probability distributions and capture function non-linearities exactly. The jackknife variance and bias estimators mimic the brute force error estimation method of comparing k completely independent MC time series of lengths T' and applying the naive estimates: removing single elements (i.e. bins) of a single time series of length T' one by one results in T' time series of length $T' - 1$, e.g. for the correlation function

estimates:

$$\begin{aligned}\hat{G}_{(s)}(i) &= \frac{1}{T' - 1} \sum_{t \neq s} \hat{G}_t(i), \\ \hat{G}_{(\cdot)}(i) &= \frac{1}{T'} \sum_s \hat{G}_{(s)}(i),\end{aligned}\tag{22}$$

resulting in jackknife-block estimates for the correlation length of:

$$\begin{aligned}\hat{\xi}_{(s)}(i) &= \Delta \left[\ln \frac{\hat{G}_{(s)}(i) - \hat{G}_{(s)}(i - \Delta)}{\hat{G}_{(s)}(i + \Delta) - \hat{G}_{(s)}(i)} \right]^{-1}, \\ \hat{\xi}_{(\cdot)}(i) &= \frac{1}{T'} \sum_s \hat{\xi}_{(s)}(i).\end{aligned}\tag{23}$$

Then the jackknife estimate of variance is given by:

$$\widehat{\text{VAR}}(\hat{\xi}(i)) = \frac{T' - 1}{T'} \sum_{s=1}^{T'} \left(\hat{\xi}_{(s)}(i) - \hat{\xi}_{(\cdot)}(i) \right)^2.\tag{24}$$

Note the missing factor of $1/(T' - 1)^2$ as compared to the usual variance estimate which accounts for the trivial correlation between the T' jackknife-block estimates. One can show that this estimator, apart from the reweighting prefactor $(T' - 1)/T'$, is strictly conservative, i.e. deviations from the true variance are always positive⁵⁰. Similarly, the resampling scheme provides an estimate for the bias of estimators, namely:

$$\widehat{\text{BIAS}}(\hat{\xi}(i)) = (T' - 1)(\hat{\xi}_{(\cdot)}(i) - \hat{\xi}(i)),\tag{25}$$

and thus offers a bias corrected correlation length estimate:

$$\tilde{\xi}(i) = T' \hat{\xi}(i) - (T' - 1) \hat{\xi}_{(\cdot)}(i).\tag{26}$$

Since in non-pathological cases the bias of an estimator vanishes with increasing length of the time series, the jackknife bias estimate provides a good check for whether the considered series are long enough to neglect bias. A jackknife error estimate for these bias-corrected estimators is possible iterating the jackknife resampling scheme to second order⁵¹.

Since Eq. (21) gives a vector of estimators for the correlation length instead of only a single one, an improved final estimate can be achieved by an average over the $\hat{\xi}(i)$. However, as for example Fig. 2 reveals, only a certain range of distances $i = i_{\min}, \dots, i_{\max}$ is suited for this purpose, where the lower bound i_{\min} results mainly from small-distance deviations as reflected by Eq. (4), whereas the large distance bound i_{\max} cuts off the region where the signal of exponential fall-off drops below the size of statistical fluctuations, so that error estimates become inaccurate and eventually the estimator Eq. (21) becomes maldefined due to negative arguments of the logarithm. A general average is given by:

$$\bar{\xi} = \sum_{i=i_{\min}}^{i_{\max}} \alpha_i \hat{\xi}(i), \quad \sum_{i=i_{\min}}^{i_{\max}} \alpha_i = 1.\tag{27}$$

The customary optimal-weight average uses estimated variances as weights for the individual elements, i.e. relative weights $\alpha_i \propto 1/\sigma^2(\hat{\xi}(i))$ that minimize the theoretical variance of the mean value. This prescription, however, neglects correlations between the individual estimates. Note that cross-correlations between adjacent estimates $\hat{\xi}(i)$ are quite large, not only because large scale fluctuations of the correlation functions are dominant, but also since the used estimator Eq. (21) explicitly introduces such correlations increasing in range with increasing Δ . As a simple variational calculation shows, for the case of correlated variables to be averaged over, one has to choose the weights according to:

$$\alpha_k = \frac{\sum_i (\Gamma^{-1})_{ik}}{\sum_{i,j} (\Gamma^{-1})_{ij}}. \quad (28)$$

to minimize the variance of the mean value. Here, $\Gamma \in \mathbb{R}_{p \times p}$, $p = i_{\max} - i_{\min} + 1$, denotes the covariance matrix of the $\hat{\xi}(i)$. Γ itself can be estimated within the jackknife resampling scheme as:

$$\begin{aligned} \widehat{\text{CORR}}_{ij} &\equiv \widehat{\text{CORR}}(\hat{\xi}(i), \hat{\xi}(j)) = \\ &= \frac{T' - 1}{T'} \sum_{s=1}^{T'} \left(\hat{\xi}_{(s)}(i) - \hat{\xi}_{(\cdot)}(i) \right) \left(\hat{\xi}_{(s)}(j) - \hat{\xi}_{(\cdot)}(j) \right). \end{aligned} \quad (29)$$

The fact that, considering Eq. (28), variance and covariance estimates directly influence the final results for the correlation lengths, gave the motivation for the quite careful statistical treatment presented above.

Finally, the selection of the regime $i = i_{\min}, \dots, i_{\max}$ can, besides the obvious eyeball method, also be done in a way based on statistical criteria. Interpreting the average Eq. (27) as a *fit* of the estimated $\hat{\xi}(i)$ values to the trivial function $f(\hat{\xi}) = \bar{\xi} = \text{const}$, the systematic deviations from the plateau regime for very small and very large distances i should be clearly reflected in quality-of-fit parameters. Thus, looking at the χ^2 distribution,

$$\hat{\chi}^2 = \sum_{i,j=i_{\min}}^{i_{\max}} (\hat{\xi}(i) - \bar{\xi})(\hat{\Gamma}^{-1})_{ij}(\hat{\xi}(j) - \bar{\xi}), \quad (30)$$

will be a good criterion for judging the “flatness” of the plateau regime $i_{\min}, \dots, i_{\max}$ included in the average. Again, as an estimator $\hat{\Gamma}$ for the covariance matrix one can use the jackknife expression $\widehat{\text{CORR}}_{ij}$. Then finding the optimal region of distances for the average is equivalent to the optimization problem $|\hat{\chi}^2/g - 1| \rightarrow \min$, with $g = i_{\max} - i_{\min} = p - 1$ denoting the number of degrees of freedom of the fit. However, this ansatz of optimization bears some uncertainties: minimizing the distance of $\hat{\chi}^2/g$ from 1 supposes that the optimal choice includes estimates $\hat{\xi}(i)$ whose dispersion around $\bar{\xi}$ is exactly reflected by the estimated variances. In view of the jackknife’s tendency to overestimate errors it might be more favorable to minimize $|\hat{\chi}^2/g|$ itself. Furthermore, considering the statistical nature of the data, the absolute minimum of $|\hat{\chi}^2/g - 1|$ sometimes happens to be an isolated

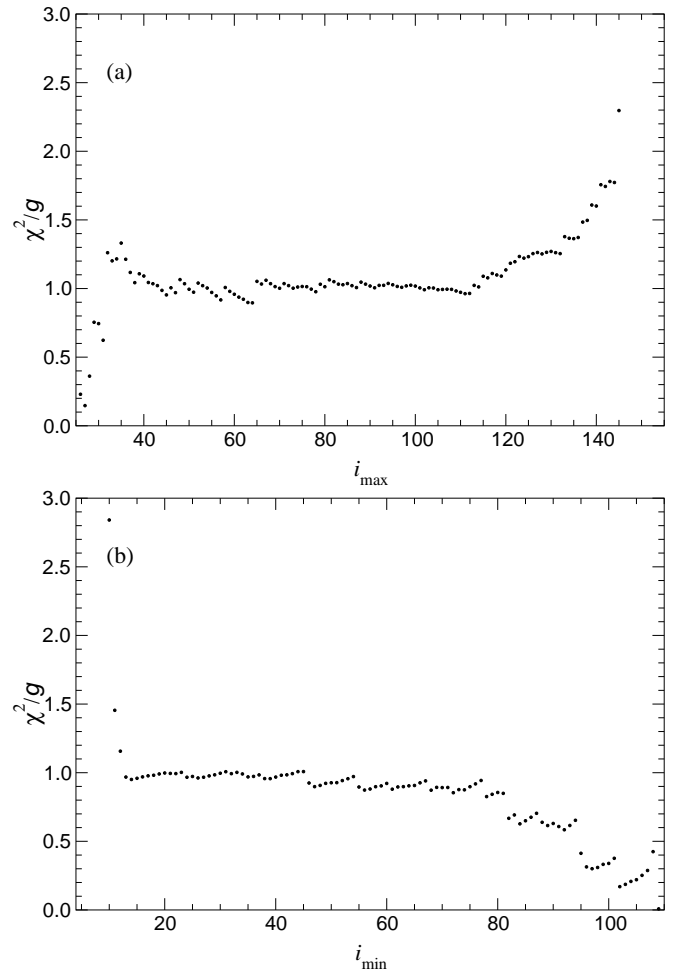


FIG. 3: Sections of $\hat{\chi}^2/g(i_{\min}, i_{\max})$ for the spin correlation length of an Ising system. (a) $\{\chi^2/g | i_{\min} = 25\}$; (b) $\{\chi^2/g | i_{\max} = 110\}$. The “wavy” structure results from $\Delta = 4$ in Eq. (21).

fluctuation, far apart from the bulk of next-to-optimal solutions. Finally, this optimization procedure tends to result in minimal values for very small regime sizes p since the fit becomes trivial for very small numbers of points; this, however, conflicts with another possible goal of optimization, namely the minimization of the overall variance of the final result. To circumvent these problems we resort to considering the whole two-dimensional distribution $\hat{\chi}^2/g(i_{\min}, i_{\max})$. It is characterized by a rather flat plateau regime for intermediate values of i_{\min} and i_{\max} and steep increases for i_{\min} becoming too small or i_{\max} becoming too large, respectively. Fig. 3 shows sections of a typical example. A good recipe for the determination of bounds is then given by first choosing a preliminary i_{\min} well above the steep ascent for small i , which was chosen to be $i_{\min} = 25$ in the example; then a plot like Fig. 3(a) allows to determine the upper bound i_{\max} , resulting in the value $i_{\max} = 110$ in the example. A plot of $\{\chi^2/g | i_{\max} = \text{const}\}$ then determines the final lower bound i_{\min} , cp. Fig. 3(b), where $i_{\min} = 17$ was

chosen. This prescription gives a method of determining the bounds in a well-defined manner that does not suffer from the drawbacks of simple minimization of $|\hat{\chi}^2/g - 1|$ mentioned above.

To test the methods of data analysis described in this section we performed simulations of the *two-dimensional* Ising model. Using a series of systems with $L_x = 5, \dots, 20$ and finite-size scaling fits including an effective higher-order correction term of the form $\xi(L_x) = AL_x + BL_x^\kappa$, we find for the leading correlation lengths scaling amplitudes $A_{\sigma/\epsilon}$ final estimates for the case of periodic boundary conditions of:

$$\begin{aligned} A_\sigma &= 1.27374(81), \\ A_\epsilon &= 0.1583(17), \end{aligned} \quad (31)$$

in excellent agreement with the exact results $A_\sigma = 4/\pi \approx 1.27324$ and $A_\epsilon = 1/2\pi \approx 0.15915$, cp. Eq. (5). For the case of antiperiodic boundary conditions we arrive at:

$$\begin{aligned} A_\sigma &= 0.42410(30), \\ A_\epsilon &= 0.07984(38), \end{aligned} \quad (32)$$

compared to CFT results of $A_\sigma = 4/3\pi \approx 0.42441$ and $A_\epsilon = 1/4\pi \approx 0.07958$, cp. Eq. (8). Note that estimates for ξ_ϵ are generally less accurate than those for ξ_σ due to the faster decay of energy-energy correlations as compared to spin-spin correlations.

IV. RESULTS: AMPLITUDE RATIOS

Let us now turn to the three-dimensional geometry $T^2 \times \mathbb{R}$ and the determination of amplitude ratios according to Eq. (6). We report the results of simulations for the $O(n)$ spin model for $n = 1, 2, 3$, and 10.

Ising Model – Simulations of the Ising model were done at an inverse temperature given by a high-precision MC estimate of the bulk critical coupling in three dimensions⁵²:

$$\beta_c = 0.2216544(3). \quad (33)$$

We use a temperature reweighting technique to check for the influence of the uncertainty of β_c on the final results^{53,54}. We find it completely negligible compared to the statistical errors for the case of the Ising model. To enable a proper FSS analysis including sub-leading terms we performed simulations for transverse system sizes $L_x = 4, 5, \dots, 20, 25$, and 30, scaling L_z accordingly. Autocorrelation times for the correlation functions are found to depend only weakly on system sizes, ranging between about 10 and 200 in units of single Wolff cluster update steps; taking the variation of the mean cluster size into account, this corresponds to one or two lattice sweeps on average. The small variation is in agreement with a dynamical critical exponent z close to zero⁵⁵. Autocorrelations of the energy-energy correlation function are generally larger by some factor of 2 than those for

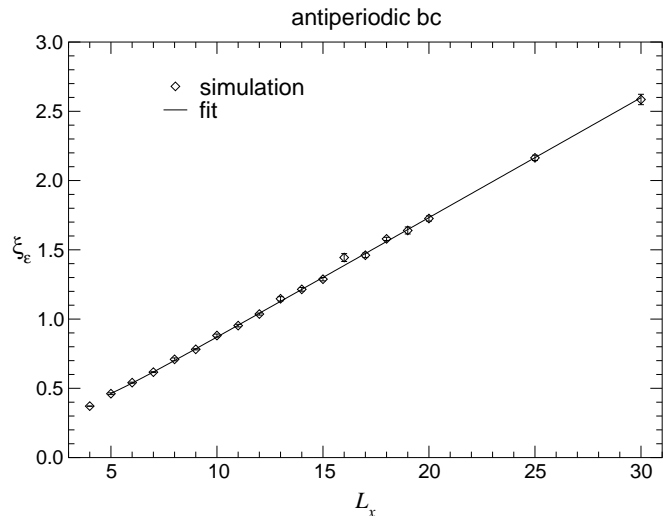


FIG. 4: Finite-size scaling of the energy-energy correlation length of the three-dimensional Ising model with antiperiodic boundary conditions. The other scaling plots look similar; we show the worst case. The fit was done to the functional form Eq. (36).

spin-spin correlations. Adapting the frequency of measurements accordingly, about 2×10^6 and 8×10^6 nearly independent measurements were recorded for the systems with periodic and with antiperiodic boundary conditions, respectively. Measurements were grouped to bins containing $2^{13} = 8192$ elements for the application of the jackknife error estimation scheme outlined in Sec. III. Collecting the final estimates $\bar{\xi}$ for the correlation lengths one ends up with a scaling plot like that shown in Fig. 4. The scaling behavior is quite linear, however, as plots of the amplitudes $\bar{\xi}/L_x$ reveal, corrections to the purely linear scaling behavior are clearly resolvable, cp. Fig. 5. As an aside, Fig. 5(b) additionally shows jackknife bias corrected estimators according to Eq. (26); for the given length of time series bias effects of our estimator Eq. (21) can clearly be neglected.

Returning to the two-dimensional case for a moment, it is easy to see the source for the leading correction term in the correlation length scaling. In the framework of conformal field theory the effect of lattice discretization as well as the influence of non-linearity of scaling fields that increase with the distance from criticality (i.e. the thermodynamic limit in our case) can be included in considerations using conformal perturbation theory¹¹. A formal perturbation expression for the spin-spin correlation length including the effect of a perturbing operator coupled with strength a_k is to first order given by

$$\xi_\sigma^{-1} = \frac{2\pi}{L} \left[x + 2\pi a_k (\mathbf{C}_{1k1} - \mathbf{C}_{0k0}) \left(\frac{2\pi}{L} \right)^{x_k-2} \right], \quad (34)$$

where the perturbing operator has dimension x_k and the coefficients \mathbf{C}_{nkn} result from the operator product expansion (OPE). One finds⁵⁶ that to lowest order the only

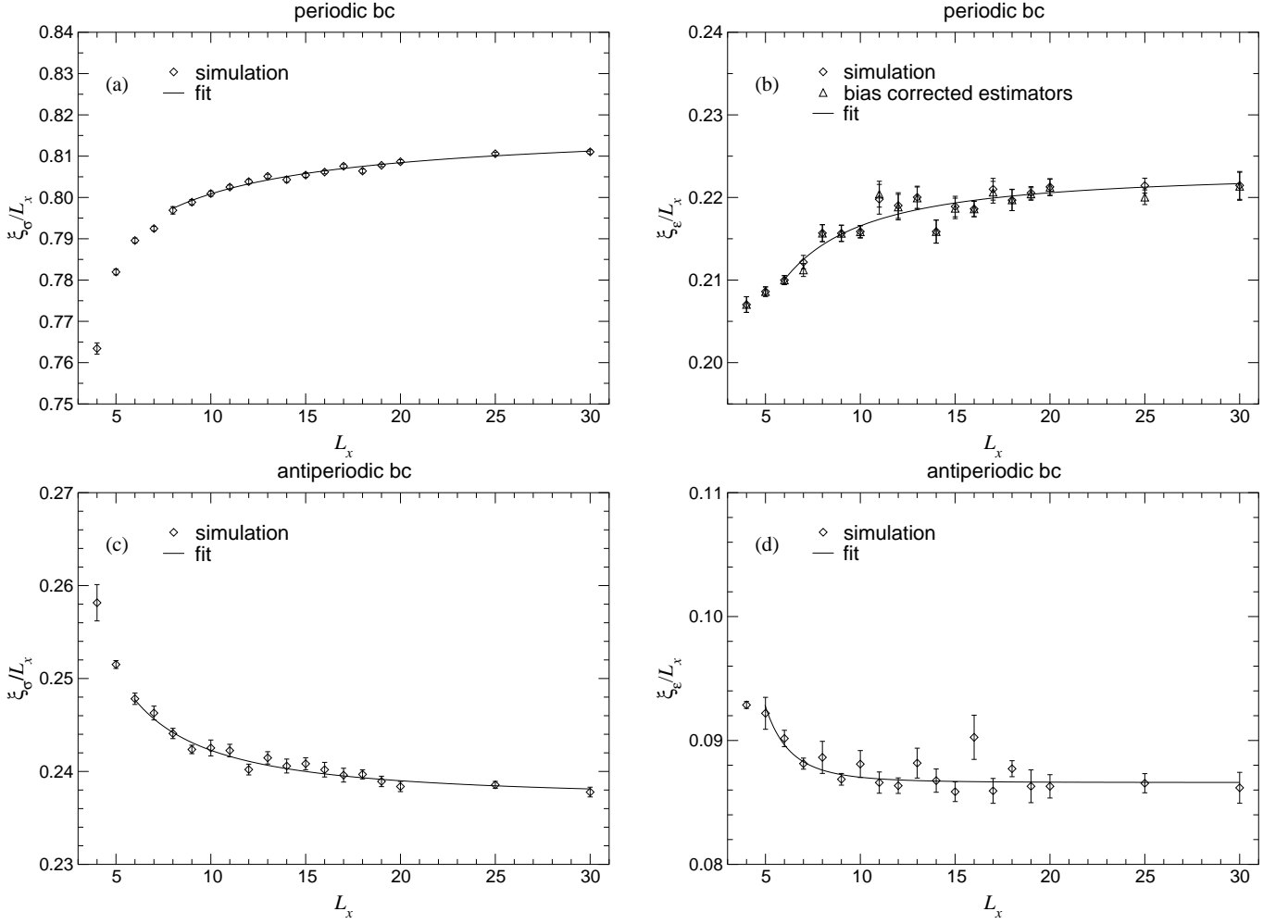


FIG. 5: Scaling of the amplitudes $\bar{\xi}_{\sigma/\epsilon}/L_x$ for the Ising model. The solid lines show fits to the function Eq. (36); (a) and (b) show correlation lengths for the systems with periodic boundary conditions, (c) and (d) for the case of an antiperiodic boundary; (b) additionally contains bias corrected estimates according to Eq. (26).

non-vanishing amplitude belongs to an operator that corresponds to the breaking of rotational symmetry by the square lattice as compared to the continuum solution. It has dimension $x_k = 4$ leading to $1/L^2$ corrections, in agreement with the first-order expansion of the exact result¹⁶:

$$\xi_{\sigma}^{-1}(L) = \frac{2\pi}{L} \left[\frac{1}{8} - 2\pi \frac{1}{768\pi} \left(\frac{2\pi}{L} \right)^2 \right]. \quad (35)$$

A similar effect will be present in the three-dimensional systems, but the correction exponent can no longer be evaluated analytically. Fig. 5 shows that the *sign* of the leading correction term is unchanged in three dimensions for the systems with periodic boundary conditions, whereas it is reversed for the systems with antiperiodic boundary. This stays true for the other $O(n)$ spin models discussed below. To account for corrections to scaling we fit the correlation lengths data to the functional form

$$\xi(L_x) = AL_x + BL_x^{\kappa}, \quad (36)$$

treating the correction exponent κ as an additional fit parameter. Due to the presence of higher-order corrections, however, the resulting values of κ have to be taken as effective exponents, that will in general differ from Wegner's correction exponent ω . Therefore we decided to keep κ as a parameter, despite of existing field-theory estimates for ω , cp.¹. We take into account the effect of neglecting higher-order correction terms by successively dropping points from the small L_x end while monitoring the quality-of-fit parameters χ^2/g resp. Q to find a compromise between fit stability and precision of the final amplitudes A . The range of sizes L_x used is indicated by the range of the solid lines in Fig. 5. Our results for the

TABLE II: Literature estimates for the inverse critical temperature β_c and the critical exponents ν and γ of the three-dimensional XY model.

Method	β_c	ν	γ
MC ⁵⁷	0.45420(2)	0.662(7)	1.308(16)
MC ⁵⁸	0.4542(1)	0.670(2)	1.319(2)
MC ⁵⁸	0.45408(8)	—	—
MC ⁵⁹	0.454165(4)	0.672(1)	1.319(2)
MC ⁶⁰	0.45421(8)	—	1.327(8)
MC ⁶¹	0.45420(2)	—	—
MC ⁶¹	0.454170(7)	—	—
MC ⁵⁷	0.454148(15)	—	—
series ⁶²	0.45406(5)	—	—
series ⁶³	0.45414(7)	—	—
series ⁶⁴	0.45420(6)	0.679(3)	1.328(6)
series ⁴⁰	0.45419(3)	0.677(3)	1.327(4)
series ⁴⁰	—	0.675(2)	1.325(3)
weighted mean	0.4541670(32)	0.6728(8)	1.3217(14)

scaling amplitudes and their ratios are:

$$\begin{aligned}
 A_\sigma &= 0.8183(32) \\
 A_\epsilon &= 0.2232(16) \quad \text{for periodic bc,} \\
 A_\sigma/A_\epsilon &= 3.666(30) \\
 A_\sigma &= 0.23694(80) \\
 A_\epsilon &= 0.08661(31) \quad \text{for antiperiodic bc.} \\
 A_\sigma/A_\epsilon &= 2.736(13)
 \end{aligned}
 \tag{37}$$

Comparing this to the ratio of scaling dimensions,

$$x_\epsilon/x_\sigma = 2.7326(16), \tag{38}$$

we find precise agreement in the sense of Eq. (6) for the case of antiperiodic boundary conditions and clear mismatch for a periodic boundary. This is in agreement with the results of Henkel²⁹ and Weston³¹, but at a level of accuracy that makes a casual coincidence very unlikely.

XY Model – The XY model is, as well as the Heisenberg models, accessible to cluster update methods using the embedded cluster representation⁴⁷, which we made use of. The simulations were performed at the coupling

$$\beta_c = 0.4541670(32), \tag{39}$$

which is an average of recent literature estimates, cp. Table II. Autocorrelation times are already noticeably larger than for the case of the Ising model; this, however, is only due to an increase of the corresponding amplitudes, the dynamic critical exponent stays on the small level of the Ising case. Using the same transverse system sizes $L_x = L_y$ as for the Ising model, but adjusting the lengths L_z according to the different correlation length amplitudes, we took between one and sixteen million

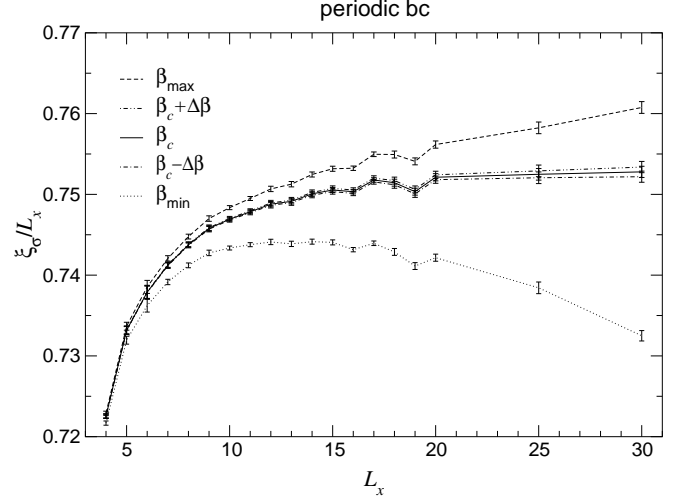


FIG. 6: Amplitude scaling of the spin-spin correlation length of the XY model with periodic boundary conditions. The spread curves show results of temperature reweighting for $\beta_c - \Delta\beta = 0.4541638$, $\beta_c + \Delta\beta = 0.4541702$, $\beta_{\min} = 0.45406$ and $\beta_{\max} = 0.45421$.

measurements, using measurement frequencies around $1/\tau_{\text{int}}$ as above. Fig. 6 shows the amplitude scaling plot of the spin-spin correlation length for periodic boundary conditions. The additional curves are results of a temperature reweighting analysis, trying to judge the effect of critical coupling uncertainties. The precision of the data is well illustrated by the fact that, reweighting our results to the minimum and maximum estimated critical couplings, respectively, cited in Table II, results in a variation of the scaling curves far beyond the range covered by the remaining statistical errors. Nevertheless, reweighting to the 1σ -range inverse temperatures $\beta_c - \Delta\beta$ and $\beta_c + \Delta\beta$ according to Eq. (39) triggers deviations at most comparable to the error estimates of the statistical analysis. The intermediate maximum of the curve for β_{\min} , however, might be an artefact indicating that β_{\min} is already too far away from the simulation temperature to allow for reliable reweighting. The effect of temperature variation is generally observed to be smaller for the antiperiodic boundary systems; furthermore, it is more important for the case of the spin-spin correlation length since here statistical errors are clearly smaller than for the energy-energy correlation length estimates. Thus, Fig. 6 shows the largest effect observed.

Fitting the final correlation length results $\bar{\xi}_{\sigma/\epsilon}$ to the functional form Eq. (36), our final estimates for the lead-

TABLE III: Literature estimates for the inverse critical temperature β_c and the critical exponents ν and γ of the three-dimensional $n = 3$ Heisenberg model.

Method	β_c	ν	γ
series ⁴⁰	0.69303(3)	0.715(3)	1.404(4)
series ⁴⁰	0.69305(4)	0.716(2)	1.406(3)
series ⁶³	0.6929(1)	0.712(10)	1.400(10)
MC ⁵⁹	0.693002(12)	0.7128(14)	1.399(2)
MC ^{65,66}	0.6930(1)	0.704(6)	1.389(14)
MC ⁶⁷	0.693035(37)	0.7036(23)	1.3896(70)
MC ⁶⁸	0.6929(1)	0.706(9)	1.390(23)
MC ⁶⁹	0.6930(2)	—	—
weighted mean	0.693004(7)	0.71187(95)	1.4008(15)

ing amplitudes and their ratios are:

$$\begin{aligned}
 A_\sigma &= 0.75409(59) \\
 A_\epsilon &= 0.1899(15) \quad \text{for periodic bc,} \\
 A_\sigma/A_\epsilon &= 3.971(32)
 \end{aligned}
 \tag{40}$$

$$\begin{aligned}
 A_\sigma &= 0.24113(57) \\
 A_\epsilon &= 0.0823(13) \quad \text{for antiperiodic bc.} \\
 A_\sigma/A_\epsilon &= 2.930(47)
 \end{aligned}$$

For a comparison with the corresponding inverse ratio of scaling dimensions we use the averaged critical exponent estimates of Table II and Eq. (11), arriving at:

$$x_\epsilon/x_\sigma = 2.923(7). \tag{41}$$

Again we find Eq. (6) confirmed for antiperiodic boundary conditions only; this behavior is obviously not specific to the Ising model.

Heisenberg Model – The $n = 3$ Heisenberg model case is treated analogously to the XY model. Table III gives the critical parameter estimates used for the simulations and comparison. With statistics similar to that for the $n = 1$ and $n = 2$ cases, but with an increase of invested computational effort due to growing autocorrelations times, the simulations confirm the findings of the Ising and XY models, cp. Table IV for details. For the case of the energy-energy correlation length of the systems with periodic boundary conditions the gathered statistics did not suffice for a stable non-linear fit including corrections according to Eq. (36). We thus performed a simple linear fit dropping the correction term. This, however, results in an error estimate which is not quite realistic and, furthermore, induces a systematic underestimation of the amplitude since one expects $B_\epsilon < 0$, cp. Fig. 5(b). From the results of the other models this effect is estimated to be about 2σ - 3σ in magnitude.

O(10) Model – To gain additional evidence and in order to facilitate considerations concerning the $n \rightarrow \infty$ limit, giving a clear picture of systematic dependencies

TABLE IV: FSS amplitudes of the correlation lengths of $O(n)$ spin models on the $T^2 \times \mathbb{R}$ geometry.

Model		periodic bc	antiperiodic bc
Ising	A_σ	0.8183(32)	0.23694(80)
	A_ϵ	0.2232(16)	0.08661(31)
	A_σ/A_ϵ	3.666(30)	2.736(13)
	x_ϵ/x_σ	2.7326(16)	
XY	A_σ	0.75409(59)	0.24113(57)
	A_ϵ	0.1899(15)	0.0823(13)
	A_σ/A_ϵ	3.971(32)	2.930(47)
	x_ϵ/x_σ	2.923(7)	
Heisenberg	A_σ	0.72068(34)	0.24462(51)
	A_ϵ	0.16966(36)	0.0793(20)
	A_σ/A_ϵ	4.2478(92)	3.085(78)
	x_ϵ/x_σ	3.091(8)	
$n = 10$	A_σ	0.671107(59)	0.25865(46)
	A_ϵ	0.1350(23)	0.07096(107)
	A_σ/A_ϵ	4.971(83)	3.645(55)
	x_ϵ/x_σ	3.661(27)	

on the parameter n , we also simulated the $n = 10$ generalized Heisenberg model. Since, of course, in the past much less effort has gone into the investigation of the $O(n)$ model with $n > 4$, there are quite few estimates of the critical coupling. We thus here use a single high-temperature series estimate of⁴⁰:

$$\beta_c = 2.42792(8). \tag{42}$$

The implementation of the Wolff cluster update algorithm has to cope with the technical intricacy of generating pseudo-random numbers equally distributed on a hyper-sphere, see Appendix A for details. Due to this complication and an again increased amplitude of the auto-correlation time scaling law we only simulated systems up to a transversal size $L_x = 20$ and reduced the number of measurements to 2×10^6 . The critical exponents for comparison are⁴⁰:

$$\nu = 0.894(4), \quad \gamma = 1.763(4). \tag{43}$$

Table IV shows again agreement between amplitude and exponent ratios only for the case of antiperiodic boundaries. Note that, as critical exponent estimates become rare with increasing n , the correlation length ratio estimate already reaches the precision of the scaling dimension ratio estimate. Checking the influence of the critical coupling uncertainty we find it only important compared to statistical errors in the case of the spin-spin correlation length for periodic boundary systems; the results reweighted to $\beta_\pm = \beta_c \pm \Delta\beta$ are $A_\sigma^- = 0.670805(56)$ and $A_\sigma^+ = 0.671432(65)$, respectively. This, however, does not noticeably influence the error of the ratio estimate, since here the error of the estimate of A_ϵ , which is much larger, is dominant.

We thus find the linear amplitude-exponent relation Eq. (6) confirmed for several spin models in three dimensions with the peculiarity that one has to insert a seam of antiferromagnetic bonds along the T^2 -directions to restore the two-dimensional situation.

V. RESULTS: “META” AMPLITUDES

Comparing our results for the three-dimensional geometry $S^1 \times S^1 \times \mathbb{R}$ to the CFT conjecture for the case of two dimensions, we are interested in the respective ranges of validity in terms of the classification of universality aspects given above in the Introduction. The fact that our simulations of the isotropic lattice representation of the $O(n)$ universality classes give results in agreement with the strongly anisotropic quantum Hamiltonian representation used by Henkel in his transfer matrix calculations for the case of the Ising model^{28,29,30}, indicates that the considered amplitude *ratios* are universal, i.e. (i') holds. Apart from that, Henkel²⁸ explicitly checked for universality of amplitude ratios by the insertion of an irrelevant perturbing operator and found it confirmed for both cases of boundary conditions. However, strictly speaking, there is no proof of universality for the cases $n > 1$. The universality aspect (i) above, i.e. universality of the amplitudes themselves, could not be checked in Henkel's calculations, because the quantum Hamiltonian is only defined up to an overall normalization constant. Yurishchev^{70,71} considered the behavior of an anisotropic Ising model and found varying correlation lengths amplitudes on variation of the ratios of couplings in the different directions. This, however, is no argument against amplitude universality since anisotropy is represented by marginal instead of irrelevant operators. On the other hand, amplitude *ratios* stay universal even with respect to those marginal perturbations, in consistency with Henkel's strongly anisotropic Hamiltonian limit calculations. In fact it is known that for all systems below their upper critical dimension at least the spin-spin correlation length scaling amplitude is an universal quantity¹⁴.

Having found very good agreement in three dimensions between ratios of correlation lengths and scaling dimensions according to Eq. (6) for the case of antiperiodic boundary conditions, it is interesting to see what the overall, operator-independent, “meta” amplitude \mathcal{A} according to:

$$\xi_{\sigma/\epsilon} = A_{\sigma/\epsilon} L_x = \frac{\mathcal{A}}{x_{\sigma/\epsilon}} L_x, \quad (44)$$

that was $\mathcal{A} = 1/2\pi$ for two-dimensional periodic systems, cp. Eq. (5), becomes in three dimensions, in particular whether it is again model independent. Since our results for the spin-spin correlation lengths are always more precise than those for energy-energy correlation lengths, we use ξ_{σ} to determine \mathcal{A} . The estimates for the spin-spin

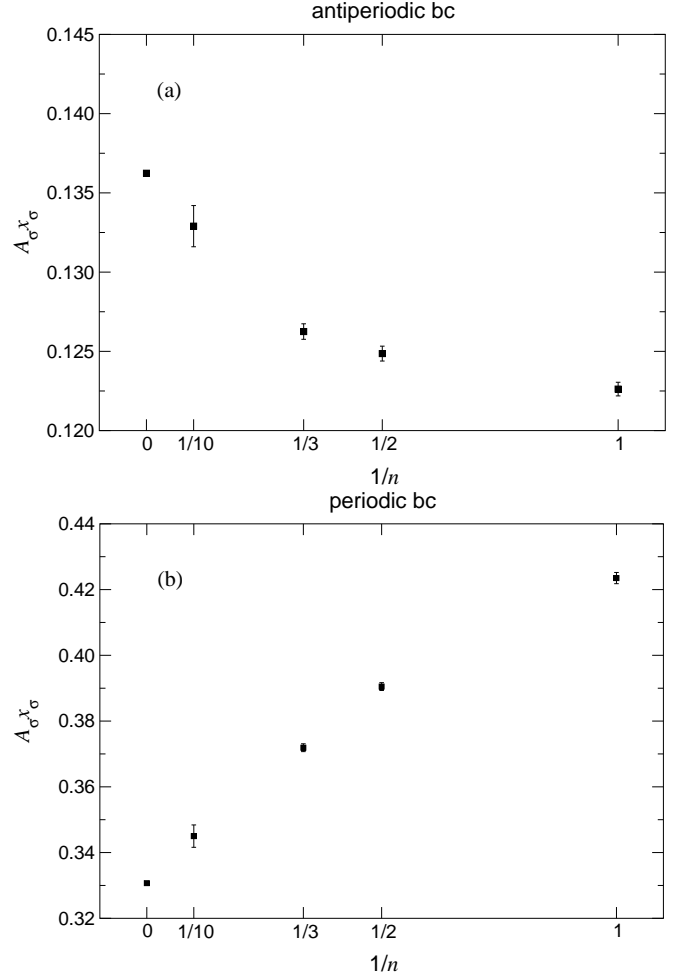


FIG. 7: (a) “Meta” amplitudes \mathcal{A} for antiperiodic boundary conditions according to Eq. (46) as a function of the order parameter dimension n ; (b) The same combination $A_{\sigma}x_{\sigma}$ for periodic boundary conditions according to Eq. (47).

scaling dimension x_{σ} resulting from the corresponding estimates of bulk critical exponents ν and γ listed in Tables I-III and Eq. (43) are:

$$x_{\sigma} = \begin{cases} 0.5175(5) & \text{Ising} \\ 0.5178(15) & \text{XY} \\ 0.5161(17) & \text{Heisenberg} \\ 0.5140(50) & n = 10 \end{cases} \quad (45)$$

Thus, inserting our results for A_{σ} listed in Table IV, we obtain for the “meta” amplitudes $\mathcal{A}(n)$:

$$\mathcal{A} = A_{\sigma}x_{\sigma} = \begin{cases} 0.12262(43) & \text{Ising} \\ 0.12486(47) & \text{XY} \\ 0.12625(49) & \text{Heisenberg} \\ 0.1329(13) & n = 10 \end{cases} \quad (46)$$

These values can additionally be compared with an analytical result that is available for the case of the spherical

model, which is commonly believed to be identical to the $n \rightarrow \infty$ limit of the $O(n)$ spin model⁷². Again using the Hamiltonian formulation, Henkel and Weston^{73,74} found that the amplitude exponent relation Eq. (6) is valid for the spherical model on $S^1 \times S^1 \times \mathbb{R}$ for *both* kinds of boundary conditions, periodic and antiperiodic. This is due to the fact that the quantum Hamiltonian factorizes into a set of uncoupled harmonic oscillators. The amplitude \mathcal{A} for the case of antiperiodic boundary conditions was found to be $\mathcal{A} \approx 0.13624$ ^{74,75}. Plotting this value together with the finite- n results of Eq. (46) shows an apparently smooth variation of the “meta” amplitudes with the order parameter dimension n , the eyeball extrapolation of the finite- n values to $1/n \rightarrow 0$ matching the spherical model result, cp. Fig. 7(a). Facing this variation, the hypothesis of a “hyperuniversal” amplitude $\mathcal{A}(n) = \mathcal{A}$ that does not depend on n , as was the case for the two-dimensional systems, can be clearly ruled out. Thus, type (iii) universality of the classification above gets broken when passing from two to three dimensions. The matching of the finite- n values with the universal spherical model amplitude, on the other hand, indicates universality also of the finite- n amplitudes and thus universality of type (i) above.

Even without a scaling law of the type Eq. (6) being valid for the case of periodic boundary conditions, one can nevertheless plot the corresponding combination $A_\sigma x_\sigma$ for this case also, as is done in Fig. 7(b). The values are:

$$A_\sigma x_\sigma = \begin{cases} 0.4235(17) & \text{Ising} \\ 0.3905(12) & \text{XY} \\ 0.3719(12) & \text{Heisenberg} \\ 0.3450(34) & n = 10 \end{cases} \quad (47)$$

The corresponding value for the spherical model is given by $A_\sigma x_\sigma \approx 0.3307$, cp.^{74,76}. The finite- n values again run smoothly into the spherical model limit, indicating amplitude universality of type (i) for periodic boundary conditions as well.

VI. THE LIMIT OF INFINITE SPIN DIMENSIONALITY

While the finite- n amplitudes of Fig. 7 fit well to the spherical model result, this is not the case for the correlation lengths ratios themselves. From inspection of Fig. 8 the smooth variation of correlation length ratios for finite n does not fit at all to the spherical model result of Henkel^{73,74} that gives a ratio $A_\sigma/A_\epsilon = 2$ for *both*, periodic and antiperiodic boundary conditions. By eyeball extrapolation one would instead expect the amplitude ratios to reach values around 4 for antiperiodic and around $5\frac{1}{3}$ for periodic boundary conditions in the limit $n \rightarrow \infty$. And indeed, accepting the validity of a linear amplitude-exponent relation according to Eq. (6) for the case of antiperiodic boundary conditions and using the usual relations for the connection between scaling dimensions and

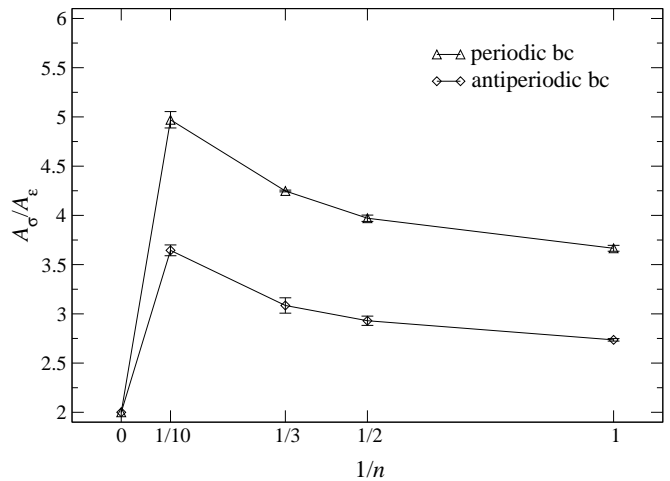


FIG. 8: Correlation lengths ratios as function of the order parameter dimension n for periodic and antiperiodic boundary conditions.

bulk critical exponents, namely Eq. (7), one would expect $x_\sigma = 1/2$ and $x_\epsilon = 2$ since $\beta = 1/2$, $\nu = 1$ and $\alpha = -1$ for the spherical model. The resulting ratio $x_\epsilon/x_\sigma = 4$ perfectly agrees with the eyeball extrapolation of our finite- n data. However, by inspection of the energy-energy correlation function in the Hamiltonian limit and using factorization arguments, Henkel⁷³ conjectured $x_\epsilon = 1$ instead, resulting in the ratio $A_\sigma/A_\epsilon = 2$, in contrast to the relation Eq. (7). Taking into account the obvious agreement of eyeball extrapolation and spherical model calculation for the amplitudes $\mathcal{A}(n)$ that were calculated from the spin-spin correlation length amplitude as $\mathcal{A}(n) = A_\sigma x_\sigma$, cp. Fig. 7, it becomes obvious that the mismatch is entirely due to the behavior of the energy-energy correlations. Note also that, since the specific heat is constant in the low-temperature phase of the spherical model in three dimensions, interpreting this as an effectively vanishing specific-heat exponent $\alpha' = 0$ leads to an effective energetic scaling dimension $x'_\epsilon = 1$.

Puzzled by this striking mismatch, we performed a roughly explorative MC simulation directly in the spherical model, which rendered results in qualitative agreement with an amplitude ratio of $A_\sigma/A_\epsilon = 2$ as suggested by the analytical calculation. Then, it is natural to ask whether there is a contradiction with Stanley’s result on the equivalence of the $n \rightarrow \infty$ limit of the $O(n)$ model and the spherical model⁷⁷, which has been, after some debate over mathematical subtleties⁷⁸, rigorously proven⁷⁹. The precise statement that can be proven is the identity of the partition functions or, equivalently, free energies of the two models in the thermodynamic limit for the whole temperature range, even independent of the order of taking the limits $n \rightarrow \infty$ and $N \rightarrow \infty$ (the thermodynamic limit). Since multi-point correlation functions do not follow from the (source-free) partition function, this does not say anything about the behavior of these functions in those two models. A direct calculation in the spherical

model, cf. Appendix B, results in a simple factorization property of the long distance behavior of the connected energy-energy correlation function for all temperatures in one and two dimensions and in the high-temperature phase down to T_c in three dimensions. If the four-point function of the spherical-model spins is denoted by C_{ijkl} , one has:

$$C_{i+1,j,j+1} - C_{ii+1}^2 = C_{ij}C_{i+1,j+1} + C_{i,j+1}C_{i+1,j} \rightarrow 2C_{ij}^2, |j-i| \rightarrow \infty, \quad (48)$$

where C_{ij} are the corresponding two-point functions. This confirms Henkel's results for the Hamiltonian formulation⁷³ on more general grounds.

Considering the $n \rightarrow \infty$ limit of the $O(n)$ model, on the other hand, reveals that the connected part of the energy-energy correlation function *vanishes* in the first-order saddle-point approximation that is being used for the comparison of the two models, cf. Appendix C. This is in agreement with general considerations for the large n model by Brézin⁷⁶. For the case of the one-dimensional spin chain, the connected energy-energy correlation function even vanishes exactly for all n , so that one can rule out an agreement of the two limits to higher order of the steepest-descent expansion in this case. Thus the mismatch of finite- n extrapolations and spherical model results of Fig. 8 has some well-defined mathematical reason.

Starting from the observation that the curves of Fig. 8 for the amplitude ratios seem to be quite parallel as a function of (finite) n for the both kinds of boundary conditions, we also plotted the collapsed ratio $\frac{A_\sigma/A_\epsilon}{x_\epsilon/x_\sigma}$ that should be unity if the amplitude-exponent relation Eq. (6) holds true. Inspecting Fig. 9, this is, according to our above results, of course the case for antiperiodic boundary conditions. Moreover, and a priori somewhat unexpected, this ratio seems to be also quite constant for the case of a periodic boundary, stabilizing around a value compatible with $4/3$ within statistical errors. Note that the exceptionally small error of the value for $n = 3$ (the Heisenberg model) and its apparent deviation towards a larger ratio is due to the impossibility to fit the $n = 3$ energy-energy correlation lengths to a scaling law including a correction term as mentioned in Sec. IV. Statistically, the data are consistent with a fit to a constant ($Q = 0.05$), and perfectly so when dropping the $n = 3$ point ($Q = 0.5$).

In view of this observation one might argue that the asymptotic scaling relation Eq. (6) in three dimensions has to be replaced by a generalized ansatz of the form

$$\frac{\xi_\sigma}{\xi_\epsilon} = R \frac{x_\epsilon}{x_\sigma}, \quad (49)$$

with an overall, model independent factor R that depends only on the boundary conditions and happens to be just 1 for the case of an antiperiodic boundary. For the amplitude scaling law this would lead to an asymptotic

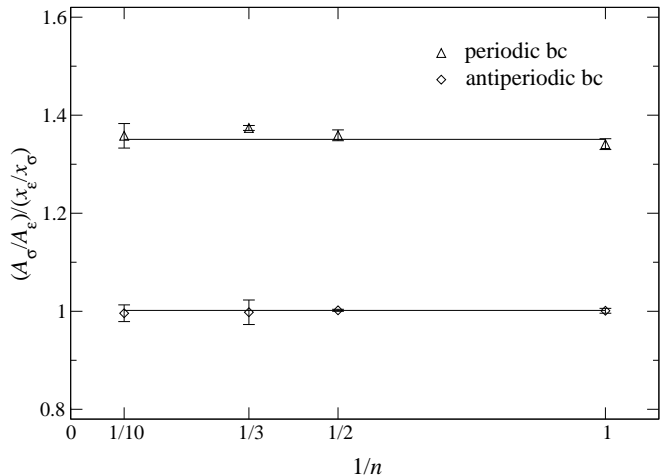


FIG. 9: Matching of correlation lengths ratios A_σ/A_ϵ and inverse scaling dimension ratios x_ϵ/x_σ for the two kinds of boundary conditions as a function of the order parameter dimension n . The horizontal lines show fits to a constant as discussed in the text.

form

$$\xi_{\sigma/\epsilon}(n) = R \frac{\mathcal{A}(n)}{x_{\sigma/\epsilon}} L_x, \quad (50)$$

cp. Eq. (5). Accepting such a generalized ansatz, a least-squares fit of the collapsed ratios of Fig. 9 to a constant R gives $R = 1.0018(18)$ for antiperiodic boundary conditions, underlining the validity of the original amplitude-exponent relation Eq. (6), or alternatively Eq. (49) with $R = 1$, for this case. For the periodic-boundary systems, on the other hand, we arrive at $R = 1.3507(74)$ (omitting the $n = 3$ point), indeed statistically consistent with the conjectured value of $4/3$.

This somewhat diminishes the at first sight apparently exceptional importance of choosing antiperiodic boundary conditions in three dimensions. Taking into account the smooth amplitude variation of Fig. 7(b) the same universality statements hold for periodic and for antiperiodic boundary conditions.

VII. CONCLUSIONS

We performed extensive MC simulations for several representatives of the class of $O(n)$ spin models. Concentrating on the geometry of three-dimensional slabs $S^1 \times S^1 \times \mathbb{R}$ we found a simple inverse linear relation between the leading scaling amplitudes of the correlation lengths of the magnetization and energy densities and the corresponding scaling dimensions valid to high accuracy for the Ising ($n = 1$), XY ($n = 2$), Heisenberg ($n = 3$), and $n = 10$ generalized Heisenberg models for *antiperiodic* boundary conditions along the torus directions. This

is the analogue of the CFT result in two dimensions with periodic boundary conditions applied. There is evidence for the universality not only of amplitude ratios (type (i')) of our classification in the Introduction), but also of scaling amplitudes themselves (type (i)). To definitely decide the question whether universality in the sense (ii) above, i.e. condensation of all operator dependent information in the scaling dimensions, is present, further operators would have to be considered. Independence, apart from changes in the scaling dimension, of the scaling amplitudes from the model under consideration, i.e. type (iii) universality, is explicitly broken for three dimensions as compared to the two-dimensional case: we find a smooth variation of the overall “meta” amplitudes $\mathcal{A}(n) = A_\sigma(n)x_\sigma(n)$, depending on the order-parameter dimension n . It might be interesting to consider further classes of models, such as for example Potts models, to see whether any of these properties are specific to the $O(n)$ spin model class.

Considering the deviation of the periodic boundary correlation lengths ratios from the corresponding inverse scaling dimension ratios, the validity of a scaling law of the form Eq. (6) can be definitely ruled out for this case. Generalizing this ansatz with an overall factor R depending on boundary conditions as in Eq. (49), however, we find it fulfilled also for the case of periodic boundaries with a factor R independent from n and taking a value compatible with $4/3$. In view of that, the fact that $R = 1$ for the case of antiperiodic boundary conditions might be rather a coincidence than a “deep” physical property. Taking into account that in two dimensions the corresponding prefactors are specific to the operators considered, cp. Eq. (8), makes it probable that a similar behavior occurs in three dimensions, destroying type (ii) universality. It might be interesting to analyze the behavior of correlation lengths in the four-dimensional geometry $S^1 \times S^1 \times S^1 \times \mathbb{R}$ to check whether a scaling law of the generalized form Eq. (49) can be retained and if so, how the factor R depends on the dimensionality of the lattice.

Trying to match our finite n results with analytical calculations for the spherical model we found a striking mismatch of the data concerning energy-energy correlations. Inspecting the four-point functions directly in the spherical model and the $O(n \rightarrow \infty)$ model limit we find that both results do not match to first order of the saddle-point approximation in general dimensions and to all orders in one dimension. Thus, the idea of equivalence of the two models has to be limited to its original extent, namely the identity of partition functions in the thermodynamic limit. Quantities not directly related to the partition function, like multi-point correlation functions, do not necessarily have to coincide. Further work has to be done to possibly evaluate exactly the correlation lengths ratios in the $n \rightarrow \infty$ limit for both sorts of boundary conditions.

Since, still, there is no explanation of the findings concerning the correlation lengths ratios for finite n in terms of a field-theoretic or otherwise exact approach, we would

like to encourage further research in this direction.

Acknowledgments

The authors thank K. Binder, J. L. Cardy, and M. Henkel for useful discussions. MW gratefully acknowledges support by the “Deutsche Forschungsgemeinschaft” through the “Graduiertenkolleg Quantenfeldtheorie”.

APPENDIX A: EQUAL DISTRIBUTION OF RANDOM NUMBERS ON A HYPER-SPHERE

Consider a probability density in polar co-ordinates $f(\phi, \theta)$ equally distributed on the 2-sphere S^2 , i.e.:

$$\frac{f(\phi, \theta) d\phi d\theta}{\sin \theta d\phi d\theta} = \text{const.} \quad (\text{A1})$$

Factorizing f as

$$f(\phi, \theta) = p(\phi) q(\theta) = \text{const} \cdot \sin \theta \quad (\text{A2})$$

and taking into account the normalization condition $\int d\Omega f(\phi, \theta) = 1$, one finds:

$$f(\phi, \theta) = p(\phi) q(\theta) = \frac{1}{2\pi} \cdot \frac{1}{2} \sin \theta. \quad (\text{A3})$$

Pseudo-random number generators usually generate numbers equally distributed in the unit interval $[0, 1]$. How does this transform to an arbitrary distribution? Let a random variable z be distributed with a density $g(z)$ and transform according to $z' = \omega(z)$; the density $h(z')$ then follows from the equation

$$g(z) dz = h(z') dz' = h(\omega(z)) \omega'(z) dz. \quad (\text{A4})$$

Thus, for random numbers z equally distributed in $[0, 1]$ the transformation:

$$\theta = \arccos(1 - 2z) \quad (\text{A5})$$

gives the desired distribution $q(\theta) = \frac{1}{2} \sin \theta$. This form is being used for the simulations of the $n = 3$ Heisenberg model.

For general polar co-ordinates in \mathbb{R}^n ,

$$\begin{aligned} x_1 &= r \cos \theta_1, \\ x_2 &= r \sin \theta_1 \cos \theta_2, \\ &\vdots \\ x_n &= r \sin \theta_1 \cdots \sin \theta_{n-1}, \end{aligned} \quad (\text{A6})$$

with $0 \leq \theta_i \leq \pi$, $0 \leq \theta_{n-1} < 2\pi$, the volume element is given by:

$$dV = r^{n-1} \sin^{n-2} \theta_1 \sin^{n-3} \theta_2 \cdots \sin \theta_{n-2} dr \prod_i d\theta_i, \quad (\text{A7})$$

so that one has for the factors $f^{(i)}(\theta_i)$ of an equally distributed density $f(\theta_1, \dots, \theta_{n-1}) = \prod_i f^{(i)}(\theta_i)$:

$$f^{(i)}(\theta_i) = \frac{1}{\gamma(n-i-1)} \sin^{n-i-1} \theta_i, \quad i < n-1, \\ f^{(n-1)}(\theta_{n-1}) = \frac{1}{2\pi}, \quad (\text{A8})$$

with normalization factors $\gamma(k) = \sqrt{\pi} \Gamma(\frac{k+1}{2}) / \Gamma(\frac{k}{2} + 1)$. Thus, for z_i equally distributed in $[0, 1]$ the transformations $z_i(\theta_i)$ are given by:

$$z_i(\theta_i) \equiv \text{int}(\theta_i) = \frac{1}{\gamma(n-i-1)} \int d\theta_i \sin^{n-i-1} \theta_i, \quad (\text{A9})$$

for $i < n-1$. The integrals can be evaluated analytically for each θ_i . There is, however, no closed form expression for the *inverse* transformation $\theta_i(z_i)$ that is needed to generate random vectors equally distributed on the hyper-sphere S^{n-1} . The trivial workaround solution of sampling equally distributed in the hyper-cube $L^n = [-1, 1] \times \dots \times [-1, 1]$, discarding the complement $L^n \setminus B^n$ and projecting the remaining points on the sphere S^{n-1} , suffers from asymptotically vanishing efficiency, since the ratio of used to discarded volumes vanishes with increasing n exponentially as $\pi^{n/2} / 2^n \Gamma(\frac{n}{2} + 1)$. We thus have to resort to a numerical inversion of $z_i(\theta_i)$. This is done by linear interpolation between a set of pre-calculated points. Using a binary-tree structure and the usual relations between the derivatives of a function and the derivatives of its inverse guarantees a constant precision of the method throughout the whole range of the z_i . Due to the monotonicity of $\text{int}(\theta_i)$ the binary trees, once set up, can just be reverted for the look-up process. Thus we reach a performance only about a factor of two worse than the analytical inversion method for the case of $n = 3$.

APPENDIX B: ENERGY-ENERGY CORRELATION FUNCTION IN THE SPHERICAL MODEL

Consider the spherical model of Berlin and Kac⁷⁷ consisting of “spins” $\epsilon_i \in \mathbb{R}$ with the constraint:

$$\sum_{i=1}^N \epsilon_i^2 = N, \quad (\text{B1})$$

where N denotes the number of lattice sites. For ease of reference we use the notation of the original paper here; thus, the ϵ_i are not to be confused with the local energy densities defined above in Eq. (15). The Hamiltonian is:

$$\mathcal{H} = -J \sum_{\langle ij \rangle} \epsilon_i \epsilon_j. \quad (\text{B2})$$

Using the Fourier representation of the δ -constraint Eq. (B1) the partition function can be written as:

$$Z_N = \frac{A_N^{-1}}{2\pi i} \int_{\alpha_0 - i\infty}^{\alpha_0 + i\infty} ds e^{Ns} \int \dots \int d\epsilon_1 \dots d\epsilon_N$$

$$\times \exp(-s \sum_i \epsilon_i^2 + K \sum_{\langle ij \rangle} \epsilon_i \epsilon_j), \quad (\text{B3})$$

choosing α_0 such that the singularities in s of the integrand are excluded from the integration volume. A_N ensures the correct normalization of the integral measure and $K = \beta J$ denotes the coupling. Diagonalizing the quadratic form $\sum_{\langle ij \rangle} \epsilon_i \epsilon_j$ with eigenvalues λ_j via an orthogonal transformation $\epsilon_i = \sum_j V_{ij} y_j$, the Gaussian integration over the ϵ_i can be performed:

$$\int \dots \int dy_1 \dots dy_N \exp[-\sum_j (s - K\lambda_j) y_j^2] \\ = \pi^{N/2} \exp[-\frac{1}{2} \sum_j \ln(s - K\lambda_j)] \quad (\text{B4})$$

so that,

$$Z_N = A_N^{-1} \pi^{N/2} 2K e^{-\frac{1}{2} N \ln 2K} \frac{1}{2\pi i} \int_{z_0 - i\infty}^{z_0 + i\infty} dz \\ \times \exp[N2Kz - \frac{1}{2} \sum_{j=1}^N \ln(z - \frac{1}{2} \lambda_j)], \quad (\text{B5})$$

where $s = 2Kz$. This expression can be evaluated in the saddle point limit $N \rightarrow \infty$ depending on the distribution of the eigenvalues λ_i for a given lattice. Now consider the two-point function,

$$C_{ij} \equiv \langle \epsilon_i \epsilon_j \rangle = \sum_{r,s} V_{ir} V_{js} \langle y_r y_s \rangle = \sum_r V_{ir} V_{jr} \langle y_r^2 \rangle, \quad (\text{B6})$$

where the last equality follows from the symmetry of the partition function Eq. (B3). Compared to the Gaussian integration Eq. (B4) the insertion of a factor y_r^2 in the integrand gives an additional factor of:

$$\frac{1}{2(s - K\lambda_r)} = \frac{1}{4K(z - \frac{1}{2} \lambda_r)}. \quad (\text{B7})$$

The corresponding integral over z can also be evaluated in the saddle point approximation⁷⁷. Now, analogously, consider the four-point function:

$$C_{ijkl} \equiv \langle \epsilon_i \epsilon_j \epsilon_k \epsilon_l \rangle = \sum_{r,s,t,u} V_{ir} V_{js} V_{kt} V_{lu} \langle y_r y_s y_t y_u \rangle. \quad (\text{B8})$$

Here, again, only paired occurrences of the y_m survive due to the inversion symmetry:

$$C_{ijkl} = \sum_r V_{ir} V_{jr} V_{kr} V_{lr} \langle y_r^4 \rangle \\ + \sum_{r \neq s} V_{ir} V_{jr} V_{ks} V_{ls} \langle y_r^2 y_s^2 \rangle \\ + \sum_{r \neq s} V_{ir} V_{js} V_{kr} V_{ls} \langle y_r^2 y_s^2 \rangle \\ + \sum_{r \neq s} V_{ir} V_{js} V_{ks} V_{lr} \langle y_r^2 y_s^2 \rangle. \quad (\text{B9})$$

The insertion of y_r^4 under the Gaussian integral gives an additional factor of:

$$\frac{3}{4(s - K\lambda_r)^2} = \frac{3}{16K^2(z - \frac{1}{2}\lambda_r)^2}, \quad (\text{B10})$$

whereas $y_r^2 y_s^2$ gives:

$$\frac{1}{16K^2(z - \frac{1}{2}\lambda_r)(z - \frac{1}{2}\lambda_s)}, \quad (\text{B11})$$

so that the diagonal terms left out in Eq. (B9) are reinserted:

$$C_{ijkl} = \sum_{r,s} (V_{ir}V_{jr}V_{ks}V_{ls} + V_{ir}V_{js}V_{kr}V_{ls} + V_{ir}V_{js}V_{ks}V_{lr}) \langle y_r^2 y_s^2 \rangle \quad (\text{B12})$$

Now performing the z -integration of Eq. (B5) in the saddle point limit $N \rightarrow \infty$ is equivalent to just inserting the saddle point value $z = z_s$ for the factors Eq. (B11), whenever a normal saddle point exists. As Berlin and Kac have shown, this is the case for all finite temperatures in one and two dimensions and for $T \geq T_c$ in three dimensions; in the low-temperature phase, the saddle point “sticks” to its value for $T = T_c$. Then, the four-point function simply factorizes, so that, comparing Eq. (B12) to the expression Eq. (B6) for the two-point function it is clear that:

$$C_{ijkl} = C_{ij}C_{kl} + C_{ik}C_{jl} + C_{il}C_{jk}, \quad (\text{B13})$$

and, finally, considering the connected energy-energy correlation function, one has:

$$C_{i+1j} - C_{ii+1}^2 = C_{ij}C_{i+1j+1} + C_{i,j+1}C_{i+1j} \rightarrow 2C_{ij}^2, \quad |j-i| \rightarrow \infty, \quad (\text{B14})$$

so that the energy-energy correlation function is trivially related to the spin-spin correlation function. This especially confirms the factor-two relation $x_\epsilon/x_\sigma = 2$ between the corresponding scaling dimensions derived by Henkel using transfer matrices⁷³. The factorization property can also be seen in the grand-canonical formulation of the spherical model, the “mean” spherical model⁸⁰, where the hard constraint Eq. (B1) is being replaced by the mean constraint:

$$\langle \sum_{i=1}^N \epsilon_i^2 \rangle = -\frac{\partial \ln Z_N}{\partial s} = N, \quad (\text{B15})$$

so that one can leave out the problematic z -integration above. There has been some debate over the coincidence of the thermodynamic limit of the two models, which is now believed to be settled⁸¹.

APPENDIX C: ENERGY-ENERGY CORRELATION FUNCTION IN THE LIMIT OF INFINITE SPIN DIMENSIONALITY

The treatment of the partition function of the $O(n)$ model in the $n \rightarrow \infty$ limit is quite analogous to that of

the spherical model, cp.⁷². For the comparison of the $n \rightarrow \infty$ limit with the spherical model the constraint $\sigma_i \cdot \sigma_i = 1$ of Eq. (13) has to be replaced by $\sigma_i \cdot \sigma_i = n$. We write the partition function of the model as:

$$Z_N^{(n)}(K) = A_N^{(n)-1} \int \cdots \int d\sigma_1^{(1)} \cdots d\sigma_N^{(n)} \prod_j \delta(n - \sigma_j^2) \times \exp[K \sum_{\langle ij \rangle} \sum_\nu \sigma_i^{(\nu)} \sigma_j^{(\nu)}], \quad (\text{C1})$$

where $A_N^{(n)}$ ensures the correct normalization. Rewriting the δ -constraints to the Fourier representation, one now has to introduce N variables $\{t_i\}$, arriving at:

$$Z_N^{(n)}(K) = A_N^{(n)-1} \left(\frac{K}{2\pi i} \right)^N \int_{-\infty}^{+\infty} \cdots \int_{-\infty}^{+\infty} d\sigma_1^{(1)} \cdots d\sigma_N^{(n)} \times \int_{-i\infty}^{+i\infty} \cdots \int_{-i\infty}^{+i\infty} dt_1 \cdots dt_N \exp(Kn \sum_i t_i) \times \prod_{\nu=1}^n \exp(-K \sum_i t_i \sigma_i^{(\nu)2} + K \sum_{\langle ij \rangle} \sigma_i^{(\nu)} \sigma_j^{(\nu)}). \quad (\text{C2})$$

Interchanging the order of integrations one is again left with integrals of Gaussian type that are easily solved transforming the spin variables orthogonally according to $\sigma_i^{(\nu)} = \sum_j V_{ij} y_j^{(\nu)}$. Note that the transformation is symmetric in the component index ν of the spins. The calculation is given in more detail for the case of a one-dimensional chain below. Here, we again consider the relation between two-point and four-point correlation functions. We take the two-point function to be

$$C_{ij} \equiv \frac{1}{n} \langle \sigma_i \cdot \sigma_j \rangle = \langle \sigma_i^{(\nu)} \sigma_j^{(\nu)} \rangle, \quad (\text{C3})$$

where the last equation for any $\nu = 1, \dots, n$ follows from the $O(n)$ symmetry of the model in the unbroken, high-temperature phase. Using the same arguments of Gaussian integration as for the case of the spherical model, the four-point function:

$$C_{ijkl} \equiv \frac{1}{n^2} \langle (\sigma_i \cdot \sigma_j)(\sigma_k \cdot \sigma_l) \rangle, \quad (\text{C4})$$

again decomposes in terms of the diagonal variables $y_i^{(\nu)}$ as:

$$C_{ijkl} = \frac{1}{n^2} \sum_{r,t,\mu,\nu} V_{ri}V_{rj}V_{tk}V_{tl} \langle y_r^{(\mu)2} y_t^{(\nu)2} \rangle + \frac{1}{n^2} \sum_{r,s,\mu} V_{ri}V_{sj}V_{rk}V_{sl} \langle y_r^{(\mu)2} y_s^{(\mu)2} \rangle + \frac{1}{n^2} \sum_{r,s,\mu} V_{ri}V_{sj}V_{sk}V_{rl} \langle y_r^{(\mu)2} y_s^{(\mu)2} \rangle \quad (\text{C5})$$

In the saddle point limit, which now corresponds to $n \rightarrow \infty$, this expression factorizes in terms of two-point functions as:

$$C_{ijkl} = C_{ij}C_{kl} + \frac{1}{n}C_{ik}C_{jl} + \frac{1}{n}C_{il}C_{jk}, \quad (\text{C6})$$

so that the “mixed” terms are suppressed with $1/n$. This asymmetry results from the preset pairing of the spin component indices μ and ν in the four-point function. As a consequence, the connected part of the energy-energy correlation function:

$$C_{i+1\ j\ j+1} - C_{i+1}^2 = \frac{1}{n} C_{ij} C_{i+1\ j+1} + \frac{1}{n} C_{i\ j+1} C_{j\ i+1}, \quad (\text{C7})$$

vanishes in the first-order saddle-point approximation. Thus, any non-vanishing contributions that are to be expected from our numerical results, have to come from sub-leading terms in the steepest-descent expansion. The correspondence of the $n \rightarrow \infty$ limit to the spherical model seems only to hold to leading order of the saddle-point approximation.

In the broken, low-temperature phase Eq. (C3) has to be replaced by

$$C_{ij} = \frac{1}{n} \langle \sigma_i \cdot \sigma_j \rangle \leq \max_{\nu} \langle \sigma_i^{(\nu)} \sigma_j^{(\nu)} \rangle \equiv C_{ij}^{\max}, \quad (\text{C8})$$

so that the factorization property of the four-point function Eq. (C6) becomes

$$C_{ijkl} \leq C_{ij} C_{kl} + \frac{1}{n} C_{ik}^{\max} C_{jl}^{\max} + \frac{1}{n} C_{il}^{\max} C_{jk}^{\max}, \quad (\text{C9})$$

and again the connected part of the energy-energy correlation function is $O(1/n)$, vanishing in the first-order saddle-point limit.

For the case of an one-dimensional lattice the first-order saddle-point approximation is exact as can be checked by explicit calculation. Consider an open chain of $O(n)$ spins⁸⁴. The partition function is given by the general expression Eq. (C1) with the nearest-neighbor sum $\sum_{\langle ij \rangle} \sigma_i \cdot \sigma_j$ replaced by the one-dimensional expression $\sum_i \sigma_i \cdot \sigma_{i+1}$. Following Stanley⁸², we factor out the integration over the last spin σ_N , which has the form:

$$\mathcal{Z}^{(n)}(K) = \frac{K}{2\pi i} \int \dots \int d\sigma^{(1)} \dots d\sigma^{(n)} \int_{-i\infty}^{+i\infty} du \exp[uK(n - \sum_{\nu} \sigma^{(\nu)2})] \exp[K \sum_{\nu} c_{\nu} \sigma^{(\nu)}], \quad (\text{C10})$$

where $c_{\nu} \equiv \sigma_{N-1}^{(\nu)}$. Inserting the unity factor $\exp[K\alpha_0(n - \sum_{\nu} \sigma^{(\nu)2})]$ and choosing α_0 sufficiently large to exclude the singularities, one has:

$$\mathcal{Z}^{(n)}(K) = \frac{K}{2\pi i} \int_{\alpha_0 - i\infty}^{\alpha_0 + i\infty} dv e^{vKn} \prod_{\nu} \int d\sigma^{(\nu)} \times \exp[-K(v\sigma^{(\nu)2} - c_{\nu}\sigma^{(\nu)})], \quad (\text{C11})$$

where $v \equiv u + \alpha_0$. Square completion and a change of variables $w = 2v$ gives:

$$\mathcal{Z}^{(n)}(K) = \left(\frac{2\pi}{K}\right)^{n/2} \frac{K}{4\pi i} \int_{2\alpha_0 - i\infty}^{2\alpha_0 + i\infty} dw \exp\left[\frac{1}{2}nK(w + 1/w)\right] w^{-n/2}, \quad (\text{C12})$$

which is an integral representation of the modified Bessel function of the first kind:

$$\mathcal{Z}^{(n)}(K) = \frac{1}{2} K (2\pi/K)^{n/2} I_{n/2-1}(nK). \quad (\text{C13})$$

Thus, the spin integrations can be done successively, the full partition function being given by:

$$\mathcal{Z}_N^{(n)}(K) = [(nK/2)^{1-n/2} \Gamma(n/2) I_{n/2-1}(nK)]^{N-1}, \quad (\text{C14})$$

where the Γ function enters through the normalization factor $A_N^{(n)-1}$ and the last integration which corresponds to $\mathcal{Z}^{(n)}(0)$. Considering the two-point function, an additional factor $\sigma_i \cdot \sigma_j$, $i < j$, is inserted in the integrand of Eq. (C1). Again starting the integration with the last spin σ_N , the first $N - j$ integrations are unaltered. The integration over σ_j gives additional factors of $c_{\nu}/2v$ from the Gaussian integration Eq. (C12), where now $c_{\nu} \equiv \sigma_{j-1}^{(\nu)}$, so that one is left with

$$\tilde{\mathcal{Z}}^{(n)}(K) = \frac{1}{2} K \left(\frac{2\pi}{K}\right)^{n/2} I_{n/2}(nK) \sum_{\nu} \sigma_i^{(\nu)} c_{\nu}, \quad (\text{C15})$$

and the form of the integrand for the next integrations is unchanged. The integration over σ_i adds a factor of n since c_{ν} above becomes $\sigma_i^{(\nu)}$ and $\sum_{\nu} \sigma_i^{(\nu)} \cdot \sigma_i^{(\nu)} = n$, followed by another $i - 1$ integrations of the partition-function type. Collecting terms one has:

$$\begin{aligned} \frac{1}{n} \langle \sigma_i \cdot \sigma_j \rangle &= \frac{[I_{n/2-1}(nK)]^{N-1+i-j} [I_{n/2}(nK)]^{j-i}}{[I_{n/2-1}(nK)]^{N-1}} \\ &= [I_{n/2}(nK)/I_{n/2-1}(nK)]^{j-i}. \end{aligned} \quad (\text{C16})$$

From this it is straightforward to derive the form of the four-point function by analogy:

$$\begin{aligned} \frac{1}{n^2} \langle (\sigma_i \cdot \sigma_j)(\sigma_k \cdot \sigma_l) \rangle &= \frac{[I_{n/2-1}(nK)]^{N-l} [I_{n/2}(nK)]^{l-k}}{[I_{n/2-1}(nK)]^{N-1}} \\ &\times [I_{n/2-1}(nK)]^{k-j} [I_{n/2}(nK)]^{j-i} \\ &\times [I_{n/2-1}(nK)]^{i-1} [I_{n/2-1}(nK)]^{1-N} \\ &= \left(\frac{I_{n/2}(nK)}{I_{n/2-1}(nK)}\right)^{(l-k)+(j-i)}, \end{aligned} \quad (\text{C17})$$

where $i < j < k < l$ is understood. For the special case of energy-energy correlations one has:

$$\frac{1}{n^2} \langle (\sigma_i \cdot \sigma_{i+1})(\sigma_j \cdot \sigma_{j+1}) \rangle = \left(\frac{I_{n/2}(nK)}{I_{n/2-1}(nK)}\right)^2, \quad (\text{C18})$$

which does not depend on the distance $|j - i|$. Hence the connected energy-energy correlation function vanishes exactly even for finite n in one dimension. The $n \rightarrow \infty$ limit of this expression is given by:

$$\frac{1}{n^2} \langle (\sigma_i \cdot \sigma_{i+1})(\sigma_j \cdot \sigma_{j+1}) \rangle = \frac{4K^2}{[1 + \sqrt{1 + (2K)^2}]^2}. \quad (\text{C19})$$

-
- * Electronic address: weigel@itp.uni-leipzig.de
† Electronic address: janke@itp.uni-leipzig.de
- ¹ J. Zinn-Justin, *Quantum Field Theory and Critical Phenomena* (Clarendon Press, Oxford, 1996).
 - ² L. P. Kadanoff, in *Phase Transitions and Critical Phenomena*, edited by C. Domb and M. S. Green (Academic Press, New York, 1976), Vol. 5A.
 - ³ M. E. Fisher and M. N. Barber, Phys. Rev. Lett. **28**, 1516 (1972).
 - ⁴ M. E. Fisher, Rev. Mod. Phys. **46**, 597 (1974).
 - ⁵ M. E. Barber, in *Phase Transitions and Critical Phenomena*, edited by C. Domb and J. L. Lebowitz (Academic Press, New York, 1983), Vol. 8, p. 146.
 - ⁶ K. Binder, in *Computational Methods in Field Theory*, edited by H. Gausterer and C. B. Lang (Springer, Berlin, 1992), p. 59.
 - ⁷ B. Dünweg, in *Monte Carlo and Molecular Dynamics of Condensed Matter Systems*, edited by K. Binder and C. Ciccotti (Italian Physical Society, Bologna, 1995).
 - ⁸ A. A. Belavin, A. M. Polyakov, and A. B. Zamolodchikov, Nucl. Phys. B **241**, 333 (1984).
 - ⁹ J. L. Cardy, Nucl. Phys. B **270**, 186 (1986).
 - ¹⁰ J. L. Cardy, Nucl. Phys. B **275**, 200 (1986).
 - ¹¹ M. Henkel, *Conformal Invariance and Critical Phenomena* (Springer, Berlin/Heidelberg/New York, 1999).
 - ¹² J. L. Cardy, J. Phys. A **17**, L385 (1984).
 - ¹³ R. B. Griffiths, Phys. Rev. Lett. **26**, 1479 (1970).
 - ¹⁴ V. Privman and M. E. Fisher, Phys. Rev. B **30**, 322 (1984).
 - ¹⁵ C. Domb, Adv. in Phys. **9**, 1 (1960).
 - ¹⁶ M. P. Nightingale, Physica A **83**, 561 (1976).
 - ¹⁷ B. Derrida and L. De Seze, J. Physique **43**, 475 (1982).
 - ¹⁸ P. Nightingale and H. W. J. Blöte, J. Phys. A **16**, L657 (1983).
 - ¹⁹ M. Weigel, Diploma thesis, Johannes-Gutenberg-Universität Mainz, 1998, unpublished.
 - ²⁰ J. L. Cardy, J. Phys. A **17**, L961 (1984).
 - ²¹ J. L. Cardy, in *Phase Transitions and Critical Phenomena*, edited by C. Domb and J. L. Lebowitz (Academic Press, London, 1987), Vol. 11, p. 55.
 - ²² J. M. Luck, J. Phys. A **15**, L169 (1982).
 - ²³ K. A. Penson and M. Kolb, Phys. Rev. B **29**, 2854 (1984).
 - ²⁴ S. Kobayashi and K. Nomitsu, *Foundations of Differential Geometry* (Interscience Publishers, New York/London/Sydney, 1969).
 - ²⁵ B. A. Dubrovin, A. T. Fomenko, and S. P. Novikov, *Modern Geometry – Methods and Applications* (Springer, New York, 1992), Vol. 1.
 - ²⁶ J. L. Cardy, J. Phys. A **18**, L757 (1985).
 - ²⁷ M. Weigel and W. Janke, to be published.
 - ²⁸ M. Henkel, J. Phys. A **19**, L247 (1986).
 - ²⁹ M. Henkel, J. Phys. A **20**, L769 (1987).
 - ³⁰ M. Henkel, J. Phys. A **20**, 3969 (1987).
 - ³¹ R. A. Weston, Phys. Lett. B **248**, 340 (1990).
 - ³² M. Weigel and W. Janke, Phys. Rev. Lett. **82**, 2318 (1999).
 - ³³ J. C. Guillou and J. Zinn-Justin, Phys. Rev. Lett. **39**, 95 (1977).
 - ³⁴ J. C. Guillou and J. Zinn-Justin, Phys. Rev. B **21**, 3976 (1980).
 - ³⁵ J. C. Guillou and J. Zinn-Justin, J. Physique Lett. **46**, L317 (1985).
 - ³⁶ D. B. Murray and B. G. Nickel, Technical report, Guelph University (unpublished).
 - ³⁷ J. Adler, J. Phys. A **16**, 2585 (1983).
 - ³⁸ J. H. Chen and M. E. Fisher, J. Physique **46**, 1645 (1985).
 - ³⁹ B. G. Nickel and J. J. Rehr, J. Stat. Phys. **61**, 1 (1990).
 - ⁴⁰ P. Butera and M. Comi, Phys. Rev. B **56**, 8212 (1997).
 - ⁴¹ A. M. Ferrenberg and D. P. Landau, Phys. Rev. B **44**, 5081 (1991).
 - ⁴² H. W. J. Blöte, E. Luijten, and J. R. Heringa, J. Phys. A **28**, 6289 (1995).
 - ⁴³ P. C. Hohenberg and B. I. Halperin, Rev. Mod. Phys. **49**, 435 (1977).
 - ⁴⁴ R. H. Swendsen and J.-S. Wang, Phys. Rev. Lett. **58**, 86 (1987).
 - ⁴⁵ U. Wolff, Nucl. Phys. B **334**, 581 (1990).
 - ⁴⁶ U. Wolff, Phys. Rev. Lett. **62**, 361 (1989).
 - ⁴⁷ W. Janke, in *Computational Physics*, edited by K. H. Hoffmann and M. Schreiber (Springer, Berlin, 1996), p. 10.
 - ⁴⁸ W. Janke and K. Nather, Phys. Rev. B **48**, 7419 (1993).
 - ⁴⁹ H. Flyvbjerg and H. G. Petersen, J. Chem. Phys. **91**, 461 (1989).
 - ⁵⁰ B. Efron, *The Jackknife, the Bootstrap and Other Resampling Plans* (Society for Industrial and Applied Mathematics [SIAM], Philadelphia, 1982).
 - ⁵¹ B. A. Berg, Comput. Phys. Commun. **69**, 7 (1992).
 - ⁵² A. L. Talapov and H. W. J. Blöte, J. Phys. A **29**, 5727 (1996).
 - ⁵³ A. M. Ferrenberg and R. H. Swendsen, Phys. Rev. Lett. **61**, 2635 (1988).
 - ⁵⁴ A. M. Ferrenberg and R. H. Swendsen, Phys. Rev. Lett. **63**, 1658(E) (1989).
 - ⁵⁵ U. Wolff, Phys. Lett. A **228**, 379 (1989).
 - ⁵⁶ P. Reinicke, J. Phys. A **20**, 4501 and 5325 (1987).
 - ⁵⁷ A. P. Gottlob, J. Stat. Phys. **77**, 919 (1994).
 - ⁵⁸ W. Janke, Phys. Lett. A **148**, 306 (1990).
 - ⁵⁹ H. G. Ballesteros, L. A. Fernández, V. Martín-Mayor, and A. Muñoz Sudupe, Phys. Lett. B **387**, 125 (1996).
 - ⁶⁰ M. Hasenbusch and S. Meyer, Phys. Lett. B **241**, 238 (1990).
 - ⁶¹ A. P. Gottlob and M. Hasenbusch, Physica A **201**, 593 (1993).
 - ⁶² P. Butera, M. Comi, and A. J. Guttmann, Phys. Rev. B **48**, 13987 (1993).
 - ⁶³ J. Adler, C. Holm, and W. Janke, Physica A **201**, 581 (1993).
 - ⁶⁴ P. Butera and M. Comi, Phys. Rev. B **52**, 6185 (1995).
 - ⁶⁵ C. Holm and W. Janke, Phys. Rev. B **48**, 936 (1993).
 - ⁶⁶ C. Holm and W. Janke, Phys. Lett. A **173**, 8 (1993).
 - ⁶⁷ K. Chen, A. M. Ferrenberg, and D. P. Landau, Phys. Rev. B **48**, 3249 (1993).
 - ⁶⁸ P. Peczak, A. M. Ferrenberg, and D. P. Landau, Phys. Rev. B **43**, 6087 (1991).
 - ⁶⁹ I. Dimitrović, P. Hasenfratz, J. Nager, and F. Niedermayer, Nucl. Phys. B **350**, 893 (1991).
 - ⁷⁰ M. A. Yurishchev, Phys. Rev. B **50**, 13533 (1994).
 - ⁷¹ M. A. Yurishchev, Phys. Rev. E **55**, 3915 (1997).
 - ⁷² H. E. Stanley, Phys. Rev. **176**, 718 (1968).
 - ⁷³ M. Henkel, J. Phys. A **21**, L227 (1988).
 - ⁷⁴ M. Henkel and R. A. Weston, J. Phys. A **25**, L207 (1992).
 - ⁷⁵ S. Allen and R. K. Pathria, J. Phys. A **26**, 5173 (1993).
 - ⁷⁶ E. Brézin, J. Physique **43**, 15 (1982).
 - ⁷⁷ T. H. Berlin and M. Kac, Phys. Rev. **86**, 821 (1952).

- ⁷⁸ E. Helfand, Phys. Rev. **183**, 562 (1969).
- ⁷⁹ M. Kac and C. J. Thompson, Physica Norvegica **5**, 163 (1971).
- ⁸⁰ H. W. Lewis and G. H. Wannier, Phys. Rev. **88**, 682 (1952).
- ⁸¹ C. C. Yan and G. H. Wannier, J. Math. Phys. **6**, 1833 (1965).
- ⁸² H. E. Stanley, Phys. Rev. **179**, 570 (1969).
- ⁸³ C. J. Thompson, in *Phase Transitions and Critical Phenomena*, edited by C. Domb and M. S. Green (Academic Press, New York, 1972), Vol. 2, p. 177.
- ⁸⁴ Considering a *closed* chain is technically much more intricate, cp.⁸³, but, of course, gives the same results in the thermodynamic limit $N \rightarrow \infty$.